

AD-A097 159

GEOLOGICAL SURVEY DENVER COLO

F/G 8/14

CHANGES OF THE SQ QUIET DAILY VARIATIONS OF THE GEOMAGNETIC FIELD ETC(U)
1981 W H CAMPBELL

1981 W H CAMPBELL

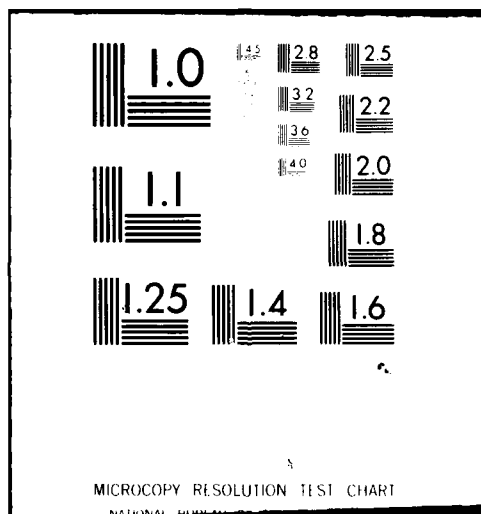
UNCLASSIFIED

NL

100

0.0000

END
DATE
FILMED
5-8
DTIC



LEVEL II

2

AD A 097159

Changes of the Sq quiet daily variations of the geomagnetic field as a function of time of year and latitude

by

10
Wallace H. Campbell

U.S.G.S. Mailstop 964
Fed. Ctr. Box 25046
Denver, Co 80225

Source: U. S. Geological Survey
Denver Federal Center
Denver, CO 80225

Government Order No. 80F0061

1981

IMP. FILE COPY

ONR Research Request No. NR 081-340/3-29-80

DTIC
ELECTE
S D
APR 1 1981
D

DISTRIBUTION STATEMENT A

Approved for public release;
Distribution Unlimited

155300 81 3 16 157

Changes of the Sq quiet daily variations of the geomagnetic
field as a function of time of year and latitude

by

Wallace H. Campbell

Abstract

An analytic representation of the quiet daily variation of the geomagnetic field, Sq, was obtained for the North American region with a mean error of less than 10% of the daily variation range. The month by month 24-, 12-, 8-, and 6-hr Fourier components of the field in H, D, and Z were found to have significant annual and semiannual changes that, in general, agreed with the expectations for ionospheric current sources for the changes. Tables and computer programs are provided from which the quiet field representation may be constructed for any selected North American location. At the equator the Sq(H) variation was over 125 gammas and showed significant equinoctial maxima. At 30° to 40°, the lowest values of Sq(H) (less than 20 gammas) were representative of the region of the ionospheric current vortex. Mid latitude Sq(D) values were about 50 gammas in range. Great enhancements of the daily field, particularly in Sq(H) and Sq(Z) occurred at high latitude with a strong summertime maximum range of about 90 gammas in Sq(H) at about 75° lat. Five-degree latitude representations of the quiet daily field change illustrate the variations occurring during the day and in different months of the year.

Accession For	
NTIS GRA&I	<input checked="checked" type="checkbox"/>
DTIC TAB	<input type="checkbox"/>
Unannounced	<input type="checkbox"/>
Justification	
By <i>Per Ltr. on file</i>	
Distribution/	
Availability Codes	
Dist	Avail and/or Special
<i>A</i>	

I. Introduction

On days that may be described as "quiet" for the solar terrestrial environment of fields and particles the magnetograms of the geomagnetic field variations at the earth's surface show regular daily changes of the field that are a few tenths to several percent of the strength of the earth's main field. Figure 1 illustrates such a Sq variation in one component of the

Figure 1. Near here

field at a mid-latitude location. The figure also shows the concurrent zenith angle χ of the sun and $(\cos\chi)^{1/2}$, called the Chapman factor, that is approximately proportional to the ionospheric ionization near 100 km for the day. The solar control of the quiet daily variation is immediately evident in the enhancement, onset, and cut-off times of the D component of the field.

Any spectral analysis of the day's variation of the magnetic field at a station on the earth's surface shows clearly defined peaks. Figures 2a and

Figure 2. Near here

2b illustrate a typical spectral composition with peaks of constantly decreasing amplitude at 24, 12, 8, and 6 hr and the absence of outstanding features at shorter periods. These spectral peaks that arise because of the dependence of Sq upon solar time provide a convenient way for decomposing the geomagnetic daily variation into analytic parts for detailed study.

The Sq pattern at a station undergoes month to month changes. The 12-month display in Figure 3 illustrates how the maxima and minima in field excursions can change in time and amplitude over the year. Both annual and semiannual variations are evident here. Such variations occur in many

geophysical phenomena of ionospheric and magnetospheric origin.

The Sq pattern changes with latitude. Figure 3 shows how different the H

Figure 3. Near here

component of field at Huancayo is from the same component at Fredericksburg or Toolangi and how the annual variation in time of minimum differs between these last two stations that are in different hemispheres. The magnetograms in the 21-June column of Figure 4 indicates how the quiet-day variation will appear

Figure 4. Near here

at a number of locations from the equator to the pole.

When the magnetic field is active (the 15-June column of Figure 4) the station magnetograms may bear little resemblance to those on the well-behaved (i.e., consistent, slowly changing) quiet days. The very best pictures of earth's quiet field behavior are obtained by a selection of data from those years that have experienced the lowest number of solar-terrestrial disturbances. Such occasions happen approximately every 11 years as a result of the solar activity cycles.

If, from each day's geomagnetic record, the average of the field strengths for the quietest days of the corresponding month are subtracted, the residuals, when averaged in lunar time, will show a lunar semidiurnal variation in phase with the atmospheric tides. (Lunar time is computed for a 24-hr duration between times of largest lunar elevation angles, called lunar noon). Figure 5 shows the lunar field variations in D component at Honolulu

Figure 5. Near here

together with the Fourier component sine waves obtained from the spectral analysis of this variation. The semidiurnal variation is the most significant component. Figure 6 illustrates how much this lunar component contributes to

Figure 6. Near here

the observed field at a midlatitude station a particular day.

The present study of Sq will be limited to a description of the 4 principal spectral components (24, 12, 8, and 6 hr) as a function of latitude with the annual and semiannual changes included. Only the North American quadrant of the earth will be considered for this representative pilot program. The quietness condition was best met in 1965, a year of extremely low geomagnetic activity from solar-terrestrial sources. The daily, 3-component (H, D, and Z) geomagnetic recordings will be separated by months from which days of particularly low activity will be selected as representative of Sq. Lunar changes will be removed. Using standard spectral analysis techniques on the data from 15 observatories the Sq field variation will be represented analytically as a function of latitude. A short computer program will be designed to reconstruct the daily field change at any location. An error analysis will determine the adequacy of such a program to represent the field values at the observatories. At the present stage of the study no attempt will be made to separate the induced internal sources from the external sources of the measured fields.

II. Background

Before I describe the analysis and results let me review, briefly, what is known of the source of the Sq variations. The best interpretation of Sq-field changes supports a model that pictures the dynamo effect of diurnal and semidiurnal tidal winds in the lower ionosphere generated, in situ, by the solar heating (Richmond, 1979). The "dynamo effect" is a term used to describe the physical process like that occurring in a hydroelectrical plant to convert energy of mechanical rotation into electricity. The thermally driven atmospheric winds transport a conducting ionosphere through the earth's main field and thereby a current is caused to flow in a direction defined by that field and the driving wind. The ease with which the current flows depends upon the conductivity of the ionosphere, a gas of charged particles which, unlike most metal conductors, has a conductivity that depends upon the density of the various charges and how they are allowed to move in the presence of the earth's field. A daily change in the electron and ion density of the atmosphere is brought about by the exposure to the sun as the earth rotates. Figure 1 showed how the solar zenith angle χ and ionization factor $(\cos\chi)^{1/2}$ changes throughout a typical day. In Figure 7 the $(\cos\chi)^{1/2}$ is

Figure 7. Near here

displayed as a function of latitude for the summer solstice, winter solstice and equinox. Note that the summer to winter difference will give an annual variation in ionization at all locations except the equator and a most extreme annual variation at the high latitudes. There is a large semiannual variation of $(\cos\chi)^{1/2}$ near the equator where the equinoctial values exceed the solstitial values because of the semiannual overhead passage of the sun.

Figure 8 illustrates the seasonal variation of χ and $(\cos\chi)^{1/2}$ at a

Figure 8. Near here

mid-latitude location. A clear annual component in the ionization is seen here. Also note the asymmetry between the maximum in the Chapman ionization factor for the summer and winter with respect to the equinoxes; such an asymmetry will necessarily introduce some semiannual component into the Sq analysis. The ionospheric winds associated with the atmospheric circulation patterns show the annual and semiannual changes in solar heating and in addition they reflect the annual and semiannual variations of changing auroral activity. Figure 9 shows the mean meridional circulation in the earth's

Figure 9. Near here

thermosphere for different activity levels. There are not too many direct measurements of the wind systems that drive the ionospheric currents; the atmosphere is too dense there for satellite observations, the few rocket measurements that have been produced are relatively instantaneous samples, and the meteor-trail studies are limited in time and number. Global pictures of the ionospheric winds are often inferred from the Sq current itself.

Near the equator the earth's main field is parallel to the earth's surface at ionospheric altitudes. This feature, combined with the more intense solar ionization and heating, leads to a unique equatorial enhancement of the Sq current system called the "equatorial eletrojet." The influence of this electrojet disappears at 15° to 20° from the equator.

Models of ionospheric current patterns associated with Sq show foci near noon at about 30° north and south latitude (Matsushita, 1967). The existence of current foci means that the ratio of the northward to eastward components of field changes rapidly with latitude near that location. Tarpley (1973) showed a seasonal variation in the location of these foci that had a large annual component with conspicuous harmonics.

The semidiurnal lunar tidal oscillations of the atmosphere drag the ionosphere through the earth's field producing another ionospheric dynamo current that is also dependent upon both the existence of day-side ionization and the field direction. Special analysis of this geomagnetic lunar variation, L, (Campbell, 1980) makes use of the fact that the lunar tidal "day" is about 50.5 min longer than the solar day. Although L is about 20 times smaller than Sq at most mid-latitude locations its contribution to the observed daily change is appreciable near the equator and poles. A proper analysis of the global characteristics of Sq should have the L removed.

The earth's dipole field extending into space is distorted by the prevailing wind of field and particles blown outward from the sun. Figure 10

Figure 10. Near here

shows the contours of the average change from the dipole field in the magnetospheric regions near the earth at quiet times. Although we consider the dipole field to be locked to the earth as it rotates, a surface location will move under the magnetospheric distortion of the type shown in Figure 10 giving a Sq-type variation not of ionospheric origin. As the earth's position with respect to the sun changes through the year we may expect an annual and semiannual change in this magnetospheric component of the surface field

measurement. For example, Figure 11 shows the seasonal variations in the midnight field levels observed at low latitudes which are consistent with the distorted nightside magnetosphere (Campbell, 1981). There is still some disagreement among geophysicists regarding the field amplitudes at the earth's surface be expected from the magnetospheric changes. It is important to realize that the sharp onset and cutoff of Sq at ionospheric sunrise and sunset (c.f., Figure 1) cannot be ascribed to any magnetospheric characteristics.

At the polar edge of the auroral zones the satellite evidence shows that there are luminous auroras even during the quiet times of solar-terrestrial activity. Such evidence means that there exists an enhanced ionization and conductivity at this particle precipitation region and some field-aligned currents between the magnetosphere and the ionosphere. The associated field changes generally have maxima in the midnight to dawn hemisphere. The auroral zone ionospheric currents connect, via the ionosphere, through the auroral zone, across the polar cap and to subauroral latitudes. The aurorally related disturbances display maxima at the equinoxes. The fluctuation of auroral currents with solar activity should give an increased error in the determination of high latitude Sq on even relatively quiet days.

For the polar-cap observatories, when the average Sq quiet-day field variation is subtracted from the records, the residual shows a variation, particularly evident in Z, that has been associated with the direction of the solar wind interplanetary magnetic field toward or away from the sun (Campbell, 1976). Because this field direction is determined as the wind leaves the sun's close environment, the earth's polar region response is called the "solar sector" effect. The surface manifestation of this effect is probably due to the small shift in position of the polar-cap quiet time Sq

currents responding to the magnetospheric tail as it interacts with the parallel solar wind field. In deriving a mean monthly quiet-day field measurement in the polar cap a balance of toward and away sector days need be included. Because this balance is not always obtained the sector effect adds some error to the $Sq(Z)$ determinations at the polar-cap observatories.

Figure 12 is a diagram of the complex array of items that can contribute

Figure 12. Near here

to the ionospheric current system. One objective of the Sq research is to determine the relative importance and predictability of these contributors. In the present study I will try to represent the quiet day variations in an analytic form with a limited number of terms and to display the expected quiet field changes in North America as a function of latitude and local time. I will try to specify the annual and semiannual changes in a way that will allow a comparison of the ionospheric and magnetospheric sources of this change.

III. The Data and Analysis Technique

A large number of the world's 1965 geomagnetic observatory records have been digitized at 2.5 min intervals and are available on computer tapes at the World Data Center A for Solar-Terrestrial Physics at Boulder, Colorado. Because this particular year was an unusually quiet one the geomagnetic records can provide a remarkably complete picture of the quietest conditions of the earth's magnetic field. From these archives, data tapes were selected that gave digital values of the northward (H), eastward declination (D), and vertical-downward (V) field components for the 15 observatories listed in Table 1. This sample of locations represented a mean longitude position of

Table 1. Near here

about 98.5° West. The first two stations of this table are considered to be at equatorial locations; the next six, at middle latitudes: the following four, at the auroral region; and the last three, at the polar cap.

The station data were arranged in geomagnetic latitude. Dip latitude is generally more effective in the equatorial region because the electrojet phenomena there are controlled by field directions in the local ionosphere. However, for the American hemisphere, the differences between dip and geomagnetic equators is negligible with respect to the scale of analysis in this present study. High latitude phenomena are better ordered in geomagnetic coordinates.

The D components of field had been recorded as angular declinations. These values were converted to eastward field strengths in gammas (1 gamma = 10^{-9} Tesla) using the usual relationship: $D(\text{gammas}) = H_0 \sin(D(\text{degrees}))$, where H_0 is the total horizontal field strength in gammas.

The observatory data were separated by month and into directional components. For each month the quietest UT days were selected by the condition that for all 8 of the 3-hr index intervals, the planetary geomagnetic activity index, Kp was less than or equal to 2+. This is the lowest value of Kp that would provide a sufficient-size sample of quiet days in each month of this analysis. For each of the 2.5 min data samples of those days, the average values were formed for the H, D, and Z components separately and called $\bar{S}q$. Obvious erratic changes, such as that near 5 UT on June 21 at Baker Lake in Figure 4 were removed from the data. The appropriate lunar tidal component (Campbell, 1980) was then subtracted and the residual was

Table 1. Observatory locations

Station	Code	UT of local MDT	Geographic degrees		Geomagnetic degrees	
			Latitude	E. Longitude	Latitude	E. Longitude
Huancayo	HU	5.02	-12.05	284.67	-0.64	354.27
Tatuoca	TT	3.23	- 1.20	311.48	9.51	21.25
Paramaribo	PA	3.68	5.82	304.78	16.93	14.83
Honolulu	HO	10.53	21.32	202.00	21.17	266.99
San Juan	SJ	4.41	18.12	293.85	29.57	3.63
Tucson	TU	7.39	32.25	249.17	40.48	312.72
Fredericksburg	FR	5.16	38.20	282.63	49.54	350.42
Victoria	VI	8.23	48.52	236.58	54.27	293.51
Sitka	SI	9.02	57.07	224.67	60.09	275.86
College	CO	9.86	64.87	212.17	64.73	256.99
Barrow	BW	10.45	71.30	203.25	68.64	241.55
Baker Lake	BL	6.40	64.33	263.97	73.81	315.98
Resolute Bay	RB	6.33	74.70	265.10	83.07	290.20
Alert	AT	4.17	82.50	297.50	85.87	167.29
Thule	TH	4.61	77.48	290.83	88.95	3.56

Note: For latitude grouping purposes, the first two stations of this list are considered to be at the equatorial locations; the next six, the middle latitudes; the following four, the auroral regions; and the last three, the polar cap. UT is given in decimal hours.

Table 2.--SOLAR-QUIET DAILY VARIATIONS OF GEOMAGNETIC FIELD H

H Direction	Geomagnetic latitude(degrees)																		
	0	5	10	15	20	25	30	35	40	45	50	55	60	65	70	75	80	85	90
24-Hr Component	Amplitude (Y)	39.0	28.3	19.9	14.0	9.6	6.1	4.9	4.3	4.4	5.7	7.8	8.8	14.5	21.0	24.9	26.2	26.8	26.2
	Phase(Max hr)	11.2	11.2	11.0	10.8	10.5	9.7	7.8	5.5	2.8	0.4	23.6	23.9	21.3	19.4	19.1	19.6	20.0	20.2
	AMP (Y)	2.8	2.1	1.6	0.8	0.7	1.7	1.0	0.2	0.9	1.3	1.9	3.4	5.0	5.3	6.7	10.0	13.8	16.3
	Max mo	6.4	6.6	7.0	7.2	2.8	2.5	2.5	10.6	8.9	8.1	6.8	6.3	6.1	6.1	5.8	5.8	5.7	5.7
	Hr change	0.2	0.3	0.5	0.5	0.4	0.8	1.5	1.9	1.6	1.2	1.2	0.9	1.3	1.4	1.0	0.4	0.2	0.3
12-Hr Component	Amplitude (Y)	23.0	15.5	10.0	6.4	4.2	3.1	3.2	3.6	4.3	5.6	6.3	6.3	5.6	8.4	14.0	16.2	11.9	6.5
	Phase(Max hr)	11.3	11.3	11.2	11.1	11.1	10.5	9.0	6.7	4.9	4.4	4.9	5.4	6.0	7.9	11.2	13.9	14.2	12.5
	AMP (Y)	0.8	1.6	1.8	1.3	0.5	0.4	0.3	0.7	1.1	0.7	0.3	1.1	1.9	2.5	4.0	5.2	4.8	2.9
	Max mo	5.0	5.9	6.3	6.4	6.2	4.0	2.5	11.8	11.3	11.0	7.9	6.4	5.9	5.0	5.1	5.3	5.5	5.2
	Hr change	0.5	0.4	0.2	0.1	0.4	1.1	1.1	0.4	1.8	2.0	1.2	0.7	0.7	0.6	0.4	0.2	0.7	2.7
8-Hr Component	Amplitude (Y)	10.0	6.7	4.4	2.9	2.0	1.5	1.7	2.0	2.6	3.4	3.5	3.0	2.4	2.7	3.2	3.6	3.3	3.3
	Phase(Max hr)	11.2	11.2	11.2	11.4	11.8	11.6	10.2	8.3	6.9	6.4	6.8	7.4	8.0	8.4	10.3	12.6	13.9	13.4
	AMP (Y)	0.9	0.6	0.6	0.4	0.2	0.3	0.4	0.2	0.2	0.6	0.8	0.7	1.0	1.4	1.4	1.6	2.1	2.1
	Max mo	2.5	3.8	5.2	6.0	7.6	7.9	7.4	8.1	7.6	5.8	5.7	6.0	6.1	6.2	6.1	5.7	5.4	5.0
	Hr change	0.7	0.5	0.5	0.9	1.8	2.0	1.0	0.5	1.5	1.6	1.1	0.8	0.9	1.1	0.9	0.2	0.1	0.6
6-Hr Component	Amplitude (Y)	5.8	3.3	1.5	0.7	0.7	0.7	0.8	1.0	1.3	1.4	1.3	1.0	0.7	1.6	2.6	3.0	2.5	1.9
	Phase(Max hr)	10.7	10.8	11.2	11.7	12.0	11.3	9.8	8.5	7.6	7.3	7.5	8.2	9.2	10.2	10.9	11.7	12.4	11.6
	AMP (Y)	1.3	0.8	0.4	0.2	0.1	0.2	0.2	0.2	0.2	0.2	0.2	0.1	0.0	0.1	0.7	1.4	1.6	1.3
	Max mo	1.6	2.0	2.5	2.5	3.5	7.6	7.6	8.1	7.6	6.4	5.5	5.5	4.0	2.5	5.0	5.5	5.7	6.3
	Hr change	0.9	0.7	0.8	0.8	1.1	1.3	1.4	1.3	1.3	1.3	1.2	0.9	0.7	0.5	0.7	0.7	0.9	1.1

Table 3. --SOLAR-QUIET DAILY VARIATIONS OF GEOMAGNETIC FIELD D

D	Direction	Geomagnetic latitude(degrees)																85	90
		0	5	10	15	20	25	30	35	40	45	50	55	60	65	70	75	80	
24-hr Component	Amplitude(Y)	5.7	5.4	5.2	5.6	7.1	8.2	8.8	9.3	9.6	10.2	10.5	10.7	11.2	12.7	14.2	17.3	21.9	24.6
	Phase(Max hr)	10.6	8.4	7.2	6.7	6.4	6.0	6.0	5.7	5.1	4.6	4.8	5.2	5.5	5.6	6.5	6.5	4.8	3.0
	AMP(Y)	2.4	1.0	2.8	3.9	4.6	5.1	4.9	5.2	5.7	5.9	6.4	7.2	7.9	7.9	8.5	10.9	14.2	13.8
	Max mo	1.3	4.9	6.0	6.1	6.1	6.1	6.0	5.9	5.9	5.9	5.9	5.6	5.7	5.7	5.7	6.0	6.0	5.9
	PHASE(hr)	4.2	3.0	2.3	1.9	1.3	0.8	0.8	0.8	0.7	0.5	0.5	0.3	0.4	0.7	0.6	0.5	0.5	0.6
	Max mo	0.6	0.5	0.4	0.4	0.4	0.4	0.4	0.9	1.3	1.6	1.9	2.0	2.5	4.8	5.5	6.0	6.1	6.1
	Y Change	1.5	1.2	1.1	0.8	1.1	1.3	1.1	1.0	0.9	1.0	0.8	0.4	0.1	0.6	1.0	2.2	3.5	3.1
	Max mo	0.8	0.6	0.6	1.2	1.9	2.1	2.1	2.2	2.4	2.6	2.6	3.1	0.3	0.5	0.9	0.9	0.6	0.4
	PHASE(hr)	1.3	1.2	1.7	1.4	0.7	0.3	0.2	0.4	0.6	0.5	0.4	0.4	0.3	0.2	0.3	0.5	0.5	0.4
	Max mo	4.0	5.4	5.7	5.6	5.4	5.2	6.0	5.8	5.3	5.3	5.2	5.2	4.9	5.0	5.8	5.9	0.0	0.2
12-hr Component	Amplitude(Y)	4.6	5.4	6.1	7.0	8.1	8.9	9.3	10.0	10.8	11.1	10.7	10.0	8.8	9.0	9.6	9.5	8.6	7.3
	Phase(Max hr)	14.6	11.7	9.7	8.7	8.3	8.0	8.0	7.9	7.8	7.8	7.9	8.1	8.1	7.5	6.6	5.9	4.8	4.5
	AMP(Y)	3.4	2.3	1.5	0.2	1.4	1.6	1.0	1.5	2.5	3.2	3.9	4.9	5.5	5.7	5.2	4.4	3.2	2.6
	Max mo	0.4	0.4	0.2	8.5	6.6	6.2	5.7	5.9	6.0	6.0	6.0	6.0	6.0	6.0	6.1	6.1	6.0	6.2
	PHASE(hr)	3.6	1.6	0.7	1.3	1.0	0.6	0.4	0.5	0.7	0.7	0.7	0.6	0.5	0.3	0.2	0.1	0.6	0.9
	Max mo	7.6	7.7	1.3	1.4	1.4	1.5	1.5	1.4	1.4	1.4	1.3	0.9	0.0	10.5	9.8	6.6	6.4	6.0
	Y Change	1.6	1.6	1.6	1.4	1.3	1.4	1.6	1.5	1.2	1.0	0.9	0.8	1.0	1.6	2.2	2.3	1.5	1.0
	Max mo	0.7	0.5	0.5	0.8	1.3	1.4	1.1	0.9	1.1	1.3	1.1	0.5	0.0	0.1	0.2	0.3	0.0	5.4
	PHASE(hr)	0.6	0.3	0.3	0.3	0.1	0.2	0.4	0.2	0.2	0.3	0.3	0.3	0.4	0.5	0.3	0.5	0.5	0.4
	Max mo	1.6	0.5	5.6	5.5	5.7	3.3	3.6	3.6	0.6	0.6	0.7	0.9	1.2	1.4	1.0	0.1	0.3	1.2
8-hr Component	Amplitude(Y)	4.2	3.6	3.4	3.9	4.8	5.2	5.0	5.4	5.9	5.8	5.0	4.0	2.9	2.6	3.2	3.8	3.3	2.5
	Phase(Max hr)	5.4	3.4	2.1	1.5	1.2	1.1	1.1	1.0	0.8	0.8	0.9	1.0	1.0	0.1	23.8	0.0	0.7	0.8
	AMP(Y)	1.0	1.4	1.3	0.7	0.1	0.2	0.5	0.4	1.0	1.4	1.4	1.4	1.4	1.8	2.4	2.8	2.3	1.5
	Max mo	11.7	0.1	0.4	0.6	4.0	3.4	2.1	4.4	6.3	6.2	6.2	6.3	6.3	5.9	5.8	5.6	5.6	6.0
	PHASE(hr)	1.8	0.1	1.2	1.5	1.3	1.2	1.1	1.0	0.9	0.8	0.7	0.6	0.4	0.3	0.4	0.5	0.5	0.9
	Max mo	6.4	1.9	0.6	0.5	0.5	0.5	0.5	0.5	0.5	0.5	0.5	0.5	0.5	10.4	10.2	10.5	10.1	10.3
	Y Change	0.7	1.0	1.4	1.5	1.4	1.2	1.4	1.2	1.0	0.9	0.8	0.7	0.5	0.3	0.5	0.4	0.3	0.2
	Max mo	5.9	0.4	0.7	0.9	1.1	1.1	0.9	1.1	1.4	1.7	2.0	2.4	2.5	1.8	1.6	1.8	2.5	2.5
	PHASE(hr)	0.5	0.3	0.4	0.4	0.1	0.2	0.1	0.3	0.4	0.3	0.3	0.4	0.5	0.2	0.2	0.3	0.3	0.9
	Max mo	2.6	3.3	4.1	4.1	4.7	0.6	0.4	0.4	0.5	0.4	0.4	0.4	0.4	0.1	3.8	3.6	3.0	2.9
6-hr Component	Amplitude(Y)	1.4	1.5	1.6	1.8	2.2	2.3	2.1	2.3	2.6	2.4	1.9	1.5	1.2	1.4	2.1	2.5	2.3	1.7
	Phase(Max hr)	6.4	6.3	5.6	4.3	3.3	3.0	2.9	2.9	2.9	3.0	3.0	3.0	2.7	2.7	2.6	3.0	3.4	2.7
	AMP(Y)	0.3	0.3	0.9	0.7	0.5	0.6	0.9	0.8	0.4	0.4	0.4	0.3	0.4	0.5	0.4	0.0	0.5	0.5
	Max mo	7.9	1.9	1.8	1.4	0.7	0.5	0.3	0.6	0.0	1.5	1.0	9.1	8.5	9.2	10.0	6.7	3.4	3.4
	PHASE(hr)	1.8	1.8	1.3	0.5	1.1	1.5	1.6	1.4	1.1	0.9	0.3	0.2	0.6	0.7	0.4	0.4	0.6	0.8
	Max mo	6.7	7.0	7.4	9.7	0.1	0.6	0.6	0.5	0.3	0.1	0.3	9.0	8.8	9.3	9.3	9.3	8.8	8.2
	Y Change	0.3	0.4	0.7	0.8	0.7	0.6	0.6	0.5	0.3	0.3	0.4	0.5	0.4	0.2	0.6	1.0	0.8	0.4
	Max mo	2.2	0.8	0.6	0.9	1.1	1.2	1.2	1.4	2.2	2.2	2.7	2.9	3.1	2.1	1.9	2.1	2.4	2.7
	PHASE(hr)	0.3	0.2	0.1	0.1	0.1	0.1	0.1	0.2	0.3	0.3	0.3	0.4	0.6	0.6	0.4	0.3	0.2	0.4
	Max mo	4.3	4.4	4.6	5.2	0.8	1.6	2.1	1.3	0.9	0.9	0.8	0.4	0.1	0.1	0.4	0.8	0.8	5.8

Table 4 .--SOLAR-QUIET DAILY VARIATIONS OF GEOMAGNETIC FIELD Z

24-hr Component	Z Direction	Geomagnetic latitude(degrees)																		
		0	5	10	15	20	25	30	35	40	45	50	55	60	65	70	75	80	85	90
24-hr Component	Amplitude(Y)	5.2	5.8	6.4	6.5	5.7	4.7	4.4	4.6	4.6	3.9	3.3	3.7	5.4	7.3	14.6	19.4	16.5	8.5	4.0
	Phase(Max hr)	3.4	1.8	0.4	0.0	0.5	0.7	0.0	23.8	23.6	22.8	21.9	20.7	20.0	20.8	0.4	3.7	4.9	5.9	6.7
	ΔZ(Y)	1.6	0.9	1.8	0.9	0.3	0.7	0.5	0.5	1.4	1.4	1.6	2.0	1.9	1.7	5.8	9.3	8.4	5.5	3.0
	Max mo	6.8	2.7	2.1	2.3	7.9	9.4	10.6	5.1	5.4	5.5	5.5	5.7	5.8	6.0	5.9	5.8	5.6	5.4	5.5
	PHASE(hr)	1.0	1.7	1.4	0.8	0.4	0.6	1.0	0.9	0.6	0.6	1.2	1.5	1.2	1.6	1.8	2.8	1.8	2.8	2.0
	Max mo	0.0	11.9	11.8	11.8	11.4	11.5	0.1	0.6	1.9	4.0	5.0	5.3	5.0	3.2	2.8	3.6	7.9	8.4	8.3
	ΔZ(Y)	1.5	1.5	1.6	1.7	1.6	1.3	1.2	0.9	0.7	0.5	0.4	0.6	0.9	1.6	3.4	4.4	3.5	1.9	1.2
	Max mo	2.4	2.6	2.6	2.6	2.4	2.1	1.9	2.0	2.2	2.1	1.6	1.2	1.2	1.1	0.9	0.9	1.0	1.0	0.8
	PHASE(hr)	0.9	0.8	0.6	0.5	0.3	0.3	0.5	0.4	0.2	0.2	0.6	0.9	0.7	1.6	1.6	0.9	1.0	0.9	0.5
	Max mo	5.1	5.1	5.1	5.0	4.7	3.1	2.5	2.1	1.3	5.0	3.6	3.6	3.9	3.8	3.6	3.2	2.2	2.5	3.5
12-hr Component	Amplitude(Y)	2.7	3.9	4.5	4.6	4.1	3.4	3.1	3.5	3.9	3.8	3.4	2.8	2.7	5.7	7.5	7.0	5.1	5.8	6.4
	Phase(Max hr)	7.7	6.7	5.8	5.5	5.8	5.9	5.7	5.6	5.6	5.4	5.5	5.8	7.0	6.6	5.5	4.0	4.5	4.9	4.7
	ΔZ(Y)	0.5	0.5	0.9	0.5	0.2	0.2	0.1	0.4	1.0	1.4	1.9	2.1	1.9	1.4	1.3	0.7	1.4	1.4	6.0
	Max mo	8.5	2.1	2.5	3.2	6.4	8.5	1.0	5.0	5.5	5.5	5.6	5.7	5.9	5.4	5.5	7.0	9.5	6.2	5.3
	PHASE(hr)	1.4	1.0	0.7	0.6	0.8	0.9	0.8	0.7	0.5	0.2	0.2	0.8	2.0	1.4	0.3	0.8	0.7	0.3	1.3
	Max mo	11.8	11.8	0.0	0.3	0.3	0.2	0.3	0.6	1.0	2.6	2.2	0.6	0.1	11.9	8.0	6.4	3.7	8.5	8.4
	ΔZ(Y)	0.6	0.9	1.1	1.1	0.8	0.6	0.5	0.5	0.3	0.1	0.3	0.6	0.8	0.6	0.7	1.1	1.7	1.3	1.1
	Max mo	1.8	2.5	2.6	2.4	2.0	1.5	1.2	1.4	1.8	2.8	0.3	0.1	0.2	1.5	1.1	5.9	5.2	5.0	5.1
	PHASE(hr)	0.6	0.5	0.3	0.1	0.1	0.2	0.2	0.3	0.3	0.2	0.3	0.7	0.8	0.9	0.9	0.9	0.3	0.6	0.9
	Max mo	5.4	5.4	5.2	4.4	1.8	1.2	1.5	1.2	0.9	1.0	1.0	0.3	5.8	5.6	0.1	0.7	1.7	2.3	1.9
8-hr Component	Amplitude(Y)	0.8	1.7	2.3	2.5	2.5	2.1	1.7	1.8	2.2	2.2	2.0	1.7	1.6	3.7	6.5	7.3	4.9	2.5	1.9
	Phase(Max hr)	5.2	6.4	7.1	7.4	7.5	7.7	7.5	7.4	7.5	7.4	7.5	7.5	7.4	6.2	5.8	6.3	7.2	8.8	10.3
	ΔZ(Y)	0.3	0.5	0.7	0.5	0.2	0.1	0.1	0.2	0.5	0.6	0.5	0.5	0.4	0.7	2.6	3.6	2.7	1.4	1.1
	Max mo	11.5	1.8	2.2	2.1	2.5	2.5	1.0	8.5	8.5	8.5	8.2	8.1	8.0	5.0	5.3	5.4	5.4	5.5	5.8
	PHASE(hr)	2.4	0.9	0.1	0.4	0.8	1.1	1.1	0.9	0.7	0.3	0.1	0.0	0.1	0.0	0.1	0.4	0.5	0.8	0.8
	Max mo	6.4	6.6	9.5	0.6	0.6	0.6	0.6	0.8	0.8	0.7	0.8	2.2	4.0	8.9	11.9	1.1	3.6	5.0	5.6
	ΔZ(Y)	0.2	0.5	0.8	0.7	0.5	0.4	0.5	0.4	0.4	0.3	0.2	0.2	0.3	0.3	0.2	0.2	0.6	0.5	0.4
	Max mo	5.9	2.7	2.6	2.4	1.9	1.0	0.6	0.8	1.6	1.8	1.4	1.4	1.3	1.3	1.4	2.5	3.0	2.9	1.9
	PHASE(hr)	0.9	0.3	0.2	0.1	0.2	0.3	0.3	0.4	0.4	0.3	0.2	0.2	0.2	0.2	0.1	0.2	0.3	0.3	0.7
	Max mo	3.1	3.6	5.2	5.7	0.3	0.1	0.0	0.2	0.5	0.7	1.1	1.5	1.3	1.4	2.7	3.3	3.6	4.8	5.6
6-hr Component	Amplitude(Y)	0.8	0.8	0.9	1.0	1.1	1.1	0.8	0.8	0.9	0.9	0.8	0.7	0.7	1.7	3.2	3.9	2.8	1.7	1.6
	Phase(Max hr)	1.4	2.0	2.3	2.6	3.0	3.6	3.5	3.0	2.4	2.3	2.2	2.8	3.2	3.2	2.0	1.7	2.0	2.9	3.5
	ΔZ(Y)	0.2	0.2	0.5	0.4	0.2	0.2	0.2	0.2	0.1	0.1	0.1	0.2	0.2	0.3	0.9	1.4	1.2	1.1	1.3
	Max mo	5.5	1.6	1.3	1.0	0.4	0.4	2.5	2.5	2.5	2.5	10.0	9.4	8.5	7.0	7.3	7.1	6.5	5.8	6.1
	PHASE(hr)	0.8	0.4	0.2	0.2	0.3	0.3	0.6	0.5	0.7	0.8	0.8	0.4	0.5	0.7	0.3	0.6	1.0	1.1	0.8
	Max mo	2.1	2.4	4.5	3.7	1.0	0.4	8.3	9.6	11.5	11.5	11.3	10.1	7.5	6.8	6.0	4.8	5.2	5.0	5.8
	ΔZ(Y)	0.2	0.3	0.4	0.4	0.3	0.2	0.1	0.1	0.1	0.1	0.2	0.4	0.3	0.1	0.3	0.6	0.5	0.2	0.4
	Max mo	2.9	2.2	1.9	1.9	1.8	1.4	1.8	2.5	3.3	3.1	2.9	2.5	2.5	1.0	1.3	1.8	2.1	1.0	0.3
	PHASE(hr)	0.8	0.9	0.7	0.3	0.2	0.2	0.3	0.2	0.2	0.1	0.2	0.1	0.6	0.9	0.5	0.1	0.2	0.1	0.1
	Max mo	0.9	0.6	0.5	0.7	1.6	2.5	2.6	2.0	1.1	0.3	3.1	1.6	0.1	0.0	0.1	0.4	5.3	5.7	1.9

annual mean of the 24-hr Fourier component of $Sq(H)$ at 20° latitude has an amplitude of 9.6 gammas that occurs at 10:30 a.m. local time.

Next, for the annual variation part of Sq , the amplitude (gammas) and phase (hr of maximum) are separated in the tables to show the annual change (gammas) of amplitude from the mean value and the "month" of occurrence of the maximum in this amplitude change. Following this is the change in hours (decimal) of the mean phase and "month" of occurrence of the maximum in this phase change. Here, the "month" is represented by a division of the year into 12 equal parts, with January 1 representing 0. A repeat of this pattern of presentation for the semiannual variations completes the six basic parts of the 24-hr component presentation. The tables then continue with similar representations for the 12-, 8-, and 6-hr field components.

In all, 40 values are used to represent the Sq quiet daily variation of one directional component at one latitude. In order that the values for every 5° be shown, a 40×19 matrix is required for each of the three components. The analytic representation of the Sq by the coefficients of the three tables provide a rather complete picture of the behavior of Sq in North America, as I shall show shortly. For an example of reading values directly for the table, let us ask how the amplitude of the 8-hr component of $Sq(H)$ changes in its annual variation at 40° latitude. From the table we read that there is only 0.2 gammas change and that this change reaches its maximum in mid August ("month"=7.6).

A first picture of the latitude change of the Sq amplitudes can be obtained from a comparison of values along a row in the tables. For example, the annual mean amplitudes in H for the 24-hr component (top row of Table 2) varies from 39.0 gammas at 11:12 a.m. at the equator to a minimum of 4.1 gammas at 5:30 a.m. at 35° latitude, then to an 85° maximum of 26.8 gammas at 8 p.m.

The next step in the processing of the data was to produce a computer program that would plot the expected S_q quiet daily variations for any desired day in the year and any location in North America, given the Tables 2, 3, and 4 as reference files. The Equation (1) uses the table form of the Fourier coefficients to reconstruct a day's values of S_q for H, D, or Z.

$$S_q(t) = \sum_{n=1}^4 (c_{no} + \sum_{q=1}^2 c_{nq} \sin(90+30q(m-M_{cnq}))) \sin(90+15n(t-(P_{no} + \sum_{q=1}^2 P_{nq} \sin(90+30q(m-M_{pnq})))))) \quad (1)$$

where: $n = 1, 2, 3$, or 4 for the period of spectral component $T = \frac{24}{n}$

$q = 1$ for annual; $q = 2$ for semiannual

$m =$ selected decimal "month" of analysis: $0 =$ Jan 1; $12 =$ Dec 31

$t =$ decimal hour of analysis, 0 to 24

$c_{no} =$ amplitude, in gammas, for annual mean level of n th component

$c_{nq} =$ amplitude, in gammas, for annual ($q=1$) or semiannual ($q=2$) variation of the n th component

$P_{no} =$ phase (decimal hr of maximum) for annual mean level of n th component

$P_{nq} =$ phase (decimal hr of maximum) for annual ($q = 1$) or semiannual ($q = 2$) variation of the n th component

$M_{cnq} =$ month of maximum for amplitude variation corresponding to n and q values

$M_{pnq} =$ month of maximum for phase variation corresponding to n and q values

The BASIC language computer program using the above formulation and Tables 2, 3, and 4 to determine the daily values of S_q at a given location and date is given in Appendices A and B.

The computed Sq changes make five assumptions. The first is that the four Fourier coefficients (24, 12, 8, and 6 hr) can adequately represent the quiet daily variation. This convenient feature occurs because the principal ionospheric current generation depends upon the diurnal changes of conductivity and winds. Global vortex patterns of such current and sudden changes in the ionosphere at sunrise and sunset are mainly responsible for the harmonics at 12, 8, and 6 hr with steadily decreasing amplitudes. Although higher harmonics are present at times, these usually are buried in a general background field level that is more like "noise" in character and contributes to the error of the analysis.

The second assumption is that the principal variations in the four Fourier components throughout the year at an observatory are the annual and semiannual changes. The second Fourier analysis provided values of the annual mean, annual variation, and semiannual variation of the four harmonic coefficients. Such variations are expected because of annual and semiannual changes that are observed in the earth's heating and ionization during its yearly path around the sun. There is also a semiannual, equinoctial interaction of the earth's magnetosphere with the solar wind. Other variation harmonics have been found in the foot locus. Longer period effects, such as those associated with the 11-yr solar cycle also occur. For the short term, one-year analysis of this study it is assumed that such changes are smaller than the annual and semiannual variations.

The third assumption is that the distribution of stations selected for the study (Table 1) could be used to represent the smoothed latitude change in the above coefficients. Of course these were the only suitable stations that could be found in this region of the earth. It was good to discover that the station coefficients change only gradually with respect to latitude (cf. Figure 13). Fortunately sufficient stations were available to reflect the

special Sq regions at the equator, mid latitudes, auroral zone, and polar cap.

The fourth assumption is that for this North American study the earth induction characteristics at the important Sq frequencies vary little between stations of adjacent geomagnetic latitude location. Certainly for induction, the longer period field changes relate to deeper conductivity regions of the earth; and these deeper regions are expected to change in a more spherically symmetrical way than the surface materials. Observatories at the same geomagnetic latitude but differing in their mid continent, coastal, or island location do present conditions under which the local induced currents will contribute in different ways to the locally measured field. The induced currents, therefore, are a major source of error in the analysis.

The fifth assumption is that the Fourier coefficients can be limited to 5° geomagnetic latitude increments and that the values for any selected observatory's latitude may be linearly interpolated from the tables of these values (Tables 2, 3 and 4). This is equivalent to an assumption that the slope of the coefficient versus latitude curve changes little over a 5° increment. Figure 13 and similar plots give some measure of confidence in this assumption.

IV. Results

The daily variations of Sq in H, D, and Z for 5° latitude increments on representative equinoctial and solstitial days (Figure 14) were computed using the full 40 coefficients of each latitude column of Tables 2, 3 and 4.. A zero

Figure 14. Near here

level represents the mean of the displayed variation. For this presentation the distance between magnetograms scales 20 gammas. Several general features

should be pointed out. In the display for $Sq(H)$ the equatorial region shows the effect of the very large eastward electrojet current causing the H component to have a range of over 100 gammas. There are clear semiannual enhancements in H during the equinoctial months of March and September. At 30° to 40° we see the lowest values of $Sq(H)$; this is near the region where the ionospheric Sq current vortex would be expected. At the high latitudes we observe the auroral zone and polar cap enhancements with maximum values in the June solstice and continued large values of field change throughout the day.

In the Figure 14 display of $Sq(D)$ note the absence of extreme enhancements at the equator and polar cap that were found for $Sq(H)$. Also note the regularity of the morning maximum and afternoon minimum at most latitudes; the transition (axis crossing) shifts from near noon to slightly earlier hours with increasing latitude.

In the Figure 14 display of $Sq(Z)$ the regularity of minimum values near midday prevails at most mid and low latitudes. A clear semiannual variation occurs at the low latitudes. The field values of $Sq(Z)$ are extremely small for the polar cap winter solstice month.

The annual values of Sq are shown in Figure 15. Recall that the plots

Figure 15. Near here

are obtained from the constant term of the Fourier series analysis for the annual and semiannual variations; that is, rows 1, 2, 11, 12, 21, 22, 31, and 32 of the Tables 2, 3, and 4. This figure represents the daily field levels about which the annual and semiannual changes occur. It is from these plots that the general latitude features of Sq are described.

The annual and semiannual amplitude variations of field are represented in Tables 2, 3, and 4 by the coefficients in rows 3, 4, 7, and 8 for the 12-hr

component; by rows 23, 24, 27, and 28 for the 8-hr component; and by rows 33, 34, 37, and 38 for the 6-hr component. A plot of these features at representative latitudes is shown in Figure 16. For $Sq(H)$ note the well

Figure 16. Near here

defined semiannual change in the 24-hr coefficient and its harmonics at the equator. The seasonal changes of H about disappear in the mid latitudes then show a dominant annual change at high latitudes. At the polar cap note how the 24-hr component dominates the amplitude changes with an annual variation. The D annual change is noticeable at all latitudes. Here again the 24-hr component at the polar cap dominates the picture. The significant feature of Z is the large annual variation of the 24-hr component at 75° latitude. For the more detailed latitude picture of the annual and semiannual variations I have presented the 24- and 12-hr components in Figures 17 and 18.

Figures 17 and 18. Near here

To evaluate the accuracy of the analytical representation of the Sq field with the limited number of coefficients I compared two sets of values. The first set, OBS (for "observations"), was composed of the hourly field values scaled from the monthly quiet-day curves representing the Sq field change at each station. As the reader may recall these values were the average of the month's quietest days with the lunar variations removed. To limit the size of the data set only the equinoctial and solstitial months were used; this selection gave 96 data points for each observatory. The second set, FIT (for "Fourier fit"), was obtained from the analytical representation of the quiet day field at the same hours on the 15th day of the selected months. All

observatory locations of Table 1 were investigated.

Figure 19c illustrates the correlation between the two sets. A high

Figure 19. Near here

correlation value means that the shape of the daily and seasonal changes in the observations and the Fourier model match quite well; that is, the relative contributions of the Fourier components is representative of the station data. The correlations for the H component were excellent except near the Sq source-current vortex region between 30° and 40° and near the auroral zone between 65° to 75° . D-component values were low near the equator. Z values were low at the auroral zone and polar region. The three stations with the best correlations for all 3 field directions were Paramaribo, Fredericksburg, and Victoria. Relatively good correlations were also obtained at Huancayo, Honolulu, and Baker Lake. The mean and median values of the correlation coefficient, all stations considered, were (respectively) 0.907 and 0.936 for H; 0.918 and 0.938 for D; and 0.809 and 0.959 for Z.

To see how the field magnitudes compared I will use the term "error" to represent the absolute value of the residual difference between the corresponding elements of the sets OBS and FIT. The mean value (MEA) of this error for each station is plotted in Figure 19a. The standard deviations, σ , of these means were linearly related to the corresponding means (coefficient of regression $r^2=0.93$) such that $\sigma=0.75$ MEA. The median values of (MED) of the errors were linearly related to the mean ($r^2=0.97$) such that $MED=0.86$ MEA.

Figure 9a shows that from the equator to 60° latitude the errors are about 2 gammas or less. At the auroral zone the errors in H reach about 12 gammas, the errors in D reach about 10 gammas, and the errors in Z reach 5.5 gammas. The Z errors are also high in the polar cap. A better representation

of these station errors is the percent error obtained from the ratio of the mean error to the range of observed field values at an observatory (Figure 19b). The largest percentage errors occur for Z between 60° and 70° latitude. Paramaribo, Fredericksburg, and Victoria have the lowest, all-over percentage errors for all three components combined whereas, Huancayo, Tatuoca, Tucson, and Baker Lake show reasonably low all all-over values of less than about 10 percent. The average percentage error for all stations was 8.0% in H, 5.9% in D and 9.6% in Z.

If the values in Figures 19a and 19c are considered the necessary measures of the analytical representation of Sq then it is possible to order the observatory records such that Victoria is best, Paramaribo and Fredericksburg are very good, and Huancayo and Baker Lake are good. For future studies on induced effects of Sq these five stations would best be used in the analysis.

If it is assumed that the error is partitioned among the various Fourier components of the analytical representation in direct proportion to the amplitude of the various components, then Figure 20 shows how the mean error

Figure 20. Near here

at each observatory (Figure 19a) is divided between the Sq annual mean, annual variation and semiannual variation. Of course, such representation is a bit artificial for two principal reasons. First, an obvious amount of the error comes from the presence in the observations of field changes with periods other than the four Fourier components. Second, the causes of annual and semiannual changes may be different enough to load the error into one or the other of these long period changes in difference to their relative Fourier amplitudes; such would be the case if solar activity affected the semiannual

change more than the annual change. Intuitively, it seems that the longer period changes are less susceptible to error. The partitioned errors give an estimate of the reliability of the seasonal changes that I personally think over-rates the magnitudes. Figure 20 indicates that the annual and semiannual variations have errors less than about 0.5 gammas in H, D, and Z at latitude below 60° . At the auroral zone and polar cap latitudes the errors are larger but, in proportion to the range of annual and semiannual changes there, the error is about the same as those at lower latitudes.

V. Concluding Remarks

The analytic representation of Sq for a year of very low solar activity was obtained from monthly mean values of field for selected quiet magnetic days. Using the diurnal and three higher harmonic terms of a Fourier analysis the coefficients were obtained to represent each Sq for the three vector directions, for each month, and at 15 selected locations principally in the North American hemisphere. The yearly behavior of these coefficients were then represented by an annual mean plus an annual and semiannual variation obtained from a second Fourier analysis. Values of all the significant terms in the analyses were then plotted as a function of geomagnetic latitude and a smoothing technique was applied to obtain tables of 40 representative values of Sq behavior for each 5° latitude increment for each fixed component. With Equation 1 these tables were used to reconstruct a picture of the daily Sq variations and their seasonal changes (Figure 14). Errors in the representation were encountered primarily because of use of a limited number of Fourier coefficients in the analysis, some random variability in the quiet natural field, smoothing of values from an uneven distribution of observatories, and differences in the contribution of induced currents to the measured field at each site. A measure of these errors was taken to be the residuals between the analytical representations and the observations. There

was a variation in the error levels at the various sites but on average the error was less than 10% of the Sq amplitude range for the stations. There was a high value (0.9) of the correlation coefficients between the analytic representations and the observations.

A comprehensive representation of Sq has been presented earlier by Matsushita (1967). His analysis was for 1958, a year of high solar-terrestrial activity. He divided the study into three longitude zones, one of which was the American region. Although both north and south latitude locations were included in 10° increments, the results above 60° latitude had been removed from the presentation. Seasonal changes were represented by 4-month group-averages for Equinox, June Solstice, and December Solstice (E, J and D) months. In that study the declination values of D were represented in degrees.

There are a number of similarities and a few differences in the results of the present and the Matsushita study. As might be expected because of the difference in solar activity levels, the Matsushita values of Sq were significantly larger. The approximate source-current focus latitude for 1965, represented by a noticeable transition in the Sq(H) form, seems to be near 35° latitude in summer and equinox but closer to 25° or 30° in winter; this is about the same latitude as the 1958 results. The shape (i.e., the relative contribution of the Fourier components) of the Sq changes in the two studies are quite similar as are the directions of change in amplitude between seasons.

The present study, in addition to its representation of a very quiet solar year, has two important features. First, the presentation of the results above 60° latitude shows the transition of Sq to the large high-latitude amplitudes with major annual changes that are largely representative of the summer-winter heating and ionization differences. The significantly

quiet solar-activity year showed the Sq(H) and Sq(Z) transition to auroral latitude behavior at about 70° . The consistency of the Sq(D) variation pattern at lower latitudes seems to be preserved at the high latitudes.

Second, a high resolution of the annual and semiannual changes is possible in the present method of analysis. These changes were separately plotted in Figures 16, 17, and 18. Olson (1970) had studied the seasonal magnetospheric configurations that could contribute to a surface Sq-type variation and plotted these surface effects at 0° , 30° , and 60° latitude. Comparing my Figure 16 with Olson's (1970) Figures 9 and 10 I find that at the equator the form of the two representations is similar for H, only the present values are about 20 times those prescribed by Olson. For equatorial Z, Olson shows no semiannual term and my present annual value seems to be in the same phase but about twice the amplitude of the magnetospheric model. The seasonal change in the equatorial midnight field levels (Figure 11) follow the magnetospheric expectations (Campbell, 1981) and also do not resemble the observed Sq. At 30° latitude the presently reported annual variation in Sq(H) is negligible in size whereas Olson shows a 4 gamma annual variation with a summer maximum. My values for Sq(Z) are larger and out of phase with his at this latitude. At 60° the phases of the compared H variations are similar but my amplitudes are about 6 times those in Olson's figures; my Z component values are out of phase with Olson's model and the amplitudes also differ considerably. The annual and semiannual changes anticipated by the magnetospheric model do not match the observed changes sufficiently to encourage an assumption that the magnetosphere is more than a minor contributor to the Sq variation.

Two final cautious reminders are appropriate. First, the field changes presented here are determined for the quiet days of a year that was itself very quiet with respect to solar activity. The ionospheric conductivity, wind

and tidal systems, and location of the auroral zone should be expected to be different on days of higher solar activity. Second, the separation of the induced internal field from the external source contributions has not been included in the present study; such separation is planned for the future.

The present results represent the best determination of the quiet geomagnetic variations, Sq, within North America to be expected as minimum field variation levels under very quiet conditions. The results illustrate the suitability of four Fourier components to describe the Sq and to detail the annual and semiannual changes of these components.

VI. Acknowledgments

I thank Bill Paulishak, Virginia Lincoln, Joe Allen and Herb Kroehl of World Data Center A for Solar-Terrestrial Physics for providing the observatory data tapes and some analysis equipment for this study. The work was funded in part by the Office of Naval Research under Research Request No. NR 081-340/3-29-80..

References

- Campbell, W. H., Polar cap geomagnetic field responses to solar sector changes, 81, 4731-4744, 1976.
- Campbell, W. H., Annual and semiannual variations of the lunar semidiurnal geomagnetic field components at North American locations, J. Geomag. Geoelectr., 32, 105-128, 1980.
- Campbell, W. H., Annual and semiannual variations of the geomagnetic field at equatorial locations, J. Atmos. Terr. Phys., 43, in press, 1981.
- Matsushita, S., Solar quiet and lunar daily variation fields, Chapter III-1, pgs 302 to 424, in "Physics of Geomagnetic Phenomena", S. Matsushita and W. H. Campbell, ed., Academic Press, New York, 1398 pgs, 1967.
- Olson, W. P., Variations in the earth's surface magnetic field from the magnetopause current system, Planet. Space Sci., 18, 1471-1484, 1970.
- Richmond, A. D., Ionospheric Wind Dynamo Theory: A Review, J. Geomag. Geoelectr., 31, 287-310, 1979.
- Roble, R. G., Thermospheric Circulation Models, EOS Trans. Ame. Geophys. Union, 62, no. 3, 29, 1981.
- Sugiura, M., B. G. Ledley, T. L. Skillman, and J. P. Heppner, Magnetospheric-field distortions observed by Ogo 3 and 5, J. Geophys. Res., 76, 7552-7565, 1971.
- Tarpley, J. D., Seasonal movement of Sq current foci and related effects in the equatorial electrojet, J. Atmos. Terr. Phys., 35, 1063-1071, 1973.

Appendix A

BASIC Program for storage of Tables 2,3, and 4 on tape file.

```

1 DISP "PROGRAM 'DATAFILE' TO LO
  AD FILE ONTO TAPE"
2 REM *FOR USE IN CREATING FIL
  E OF 50 FOURIER COEFFICIENTS
  VS LATITUDE*
3 DISP "INPUT NEW FILE ARRAY N
  AME AS F:"
4 INPUT F:
5 DISP "INPUT NUMBER OF ARRAY
  COLUMNS C"
6 INPUT C
7 DISP "INPUT NUMBER OF ARRAY
  ROWS R"
8 INPUT R
9 DISP "BEFORE RUN FIX 90 DIM
  W(R)"
30 CREATE F*,C,8*R
40 REM *FILE C COL(ROWS),R R
  OWS(ITEMS EA) WITH 8 BYTES P
  ER ROW*
50 OPTION BASE 1
60 REM *ABOVE TO START COUNT AT
  1 RATHER THAN 0*
70 ASSIGN# 1 TO F:
80 REM * ABOVE FOR BUFFER*
90 DIM W(40)
100 FOR L=1 TO C
110 DISP ""
120 DISP "NEXT R VALUES FOR COLU
  MN":L
130 FOR I=1 TO R
140 INPUT W(I)
150 NEXT I
160 BEEP
161 REM * BEEP FOR END OF DATA E
  NTRY*
170 DISP "VALUES FOR COLUMN":L
180 FOR I=1 TO R
190 DISP "W":I:"=":W(I)
191 REM *CORRECT W3=2 WITH W(3)=
  3 ON DISPLAY:PRESS 'END LINE'
  *
200 NEXT I
210 DISP "CHECK,CORRECT, THEN PR
  ESS CONT"
220 PAUSE
230 PRINT# 1,L : W()
240 REM *ABOVE LISTS ALL RECORDS
  ON TAPE*
250 DISP "END R ENTRIES"
260 NEXT L
270 ASSIGN# 1 TO *
280 REM *ABOVE CLOSSES BUFFER*
290 DISP "END FILEX DATA ARRAY"
300 END

```

Appendix B

BASIC program for plotting of Sq from tape file of Tables 2,3, and 4.

```

10 REM *SQPLOT*
20 DEF FNR(D2) = INT(D2*100+.5)
/100
30 REM *ABOVE ROUNDING FCN FOR
2 PLACES*
40 DISP "ENTER STATION NAME"
50 INPUT N$
51 PRINT N$
60 DEG
70 DISP "ENTER GEOGRAPHIC LAT. I
N DECIMAL DEG WITH NORTH +"
80 INPUT G1
90 PRINT G1;"DEG LATITUDE"
100 DISP "ENTER GEOGRAPHIC LONG
IN DECIMAL DEG WITH EAST +"
110 INPUT G2
120 PRINT G2;"DEG LONGITUDE"
130 C1=COS(11.3)
140 C2=SIN(11.3)
150 C3=COS(G2-389.6)
160 C4=SIN(G2-389.6)
170 L1=ASN(SIN(G1)*C1+COS(G1)*C2
*C3)
180 L2=ASN(COS(G1)*C4/COS(L1))
181 IF L2>=0 THEN 184
182 L2=360+L2
183 GOTO 190
184 IF L2<360 THEN 190
185 L2=L2-360
190 PRINT FNR(L1);"DEG GEOMAGNET
IC LATITUDE"
200 DISP FNR(L1);"DEG GEOMAGNETI
C LATITUDE"
210 PRINT FNR(L2);"DEG GEOMAGNET
IC LONG"
220 DISP FNR(L2);"DEG GEOMAGNETI
C LONG"
221 IF L1<0 OR L1>90 THEN 223
222 GOTO 230
223 BEEP
224 DISP "GEOMAG LAT OUTSIDE RAN
GE -SELECT NEW LOCATION AND
RUN"
225 PRINT "NO COMPUTATION"
226 PRINT " "
227 PAUSE
230 DISP "SELECTED ANALYSIS DATE
"
231 DISP "DAY=";
232 INPUT D
233 DISP "MONTH=";
234 INPUT M
237 Y=1965
238 IF M=1 OR M=2 THEN 242
239 Y1=Y
240 M1=M+1
241 GOTO 244
242 Y1=Y-1
243 M1=M+13
244 J1=0-INT(.75*INT(Y1/100)-7)+
INT(365.25*Y1)+INT(30.6*M1)
245 J2=1-INT(.75*INT((Y-1)/100)-
7)+INT(365.25*(Y-1))+INT(30.
6*M1)
246 D1=J1-J2+1
250 PRINT "DAY=";D1;"MONTH=";M;"D
AY NUMBER FOR YEAR =" ;D1
260 M1=(D1-1)/30.4167
280 DISP FNR(M1);"IS ANALYSIS MO
NTH"
290 U1=24-G2/15
291 IF U1<24 THEN 300
292 U1=U1-24
300 PRINT "UT OF LOCAL MDT =" ;FNR
R(U1)
310 DISP FNR(U1);"IS UT AT LOCAL
NOON"
320 REM *N=1,2,3,4 FOR PERIODS 2
4,12,8,6 HR WHERE T=24/N"
330 REM *P=1,2 FOR AMP(1) OF PHA
SE(2)*
340 REM *Q=1,2 FOR ANN(1) OR SEM
IANN(2)
350 L3=L1/5+1
360 REM *SELECT BRACKETING L*
370 FOR L=1 TO 19
380 IF L3>=L AND L3<L+1 THEN 400
390 NEXT L
400 DISP "LOWER TABLE LATITUDE";
5*(L-1);"DEG"
410 OPTION BASE 1
411 FOR A=1 TO 3
412 IF A=1 THEN 430
413 IF A=2 THEN 432
414 IF A=3 THEN 434
430 ASSIGN# 1 TO "SOHLAT"
431 C$="H" @ GOTO 440
432 ASSIGN# 1 TO "SOQLAT"
433 C$="Q" @ GOTO 440
434 ASSIGN# 1 TO "SOZLAT"
435 C$="Z" @ GOTO 440
440 DIM W(40)
441 DIM H3(40)
442 DIM Y(40)
443 DIM H(19,40)
450 FOR X=L TO L+1
460 READ# 1,X ; W()
461 DISP "VALUES AT LAT";FNR(5*(
X-1))
470 FOR I=1 TO 40
480 H(X,I)=W(I)
490 DISP H(X,1)
500 NEXT I
510 NEXT X
550 FOR X=1 TO 40
551 Y(X)=H(L+1,X)-H(L,X)
560 IF X=2 OR X=12 OR X=22 OR X=
32 THEN 580
570 GOTO 640
580 IF Y(X)>=12 THEN 610
590 IF Y(X)<=-12 THEN 630

```

```

600 GOTO 631
610 Y(X)=Y(X)-24
620 GOTO 631
630 Y(X)=Y(X)+24
631 H3(X)=(L3-L)*Y(X)+H(L,X)
632 IF H3(X)>0 THEN 830
633 H3(X)=H3(X)+24
634 GOTO 830
640 IF X=4 OR X=6 OR X=14 OR X=1
    6 OR X=24 OR X=26 OR X=34 OR
    X=36 THEN 660
650 GOTO 730
660 IF Y(X)>=6 THEN 690
670 IF Y(X)<=-6 THEN 710
680 GOTO 711
690 Y(X)=Y(X)-12
700 GOTO 711
710 Y(X)=Y(X)+12
711 H3(X)=(L3-L)*Y(X)+H(L,X)
712 IF H3(X)>0 THEN 830
713 H3(X)=H3(X)+12
714 GOTO 830
720 GOTO 820
730 IF X=8 OR X=10 OR X=18 OR X=
    20 OR X=28 OR X=30 OR X=38 O
    R X=40 THEN 750
740 GOTO 820
750 IF Y(X)>=3 THEN 780
760 IF Y(X)<=-3 THEN 800
770 GOTO 801
780 Y(X)=Y(X)-6
790 GOTO 801
800 Y(X)=Y(X)+6
801 H3(X)=(L3-L)*Y(X)+H(L,X)
802 IF H3(X)>0 THEN 830
803 H3(X)=H3(X)+6
804 GOTO 830
810 GOTO 820
820 H3(X)=(L3-L)*Y(X)+H(L,X)
830 REM *ABOVE GIVES INTERPOLATE
    D VALUES*
840 DISP "TAB VAL":FNR(X):"=":FNR
    (H3(X))
850 NEXT X
860 ASSIGN# 1 TO *
870 REM *NOW HAVE 40 INTERPOLATE
    D VALUES OF TABLE FOR GEOMAG
    LAT L1*
880 REM *N=PERIOD SELECT SO T=24
    /N*
891 REM *R=1 FOR AMP; 2 FOR PHAS
    E*
902 REM *Q=1 FOR ANN; 2 FOR SEMI
    ANN*
883 REM *N1= MONTH VALUE*
884 REM *F(N,R) AND F1(Q)
920 DEG
930 DIM F(4,2)
940 DIM F1(2)
950 FOR N=1 TO 4

```

```

960 FOR R=1 TO 2
970 FOR Q=1 TO 2
980 F1=2*R-2
990 F1(Q)=H3(3+R1+4*(Q-1)+10*(N-
    1))*SIN(30*Q*(M1-H3(4+R1+4*(
    Q-1)+10*(N-1)))+90)
1000 NEXT Q
1010 F(N,R)=F1(1)+F1(2)
1011 DISP "F("N";","R")=":FNR(
    F(N,R))
1020 NEXT R
1030 NEXT N
1040 DIM H4(241)
1050 DIM K(4)
1060 FOR N=1 TO 4
1070 FOR R=1 TO 2
1080 F(N,R)=F(N,R)+H3(R+10*(N-1)
    )
1090 DISP "TOT F("N";","R")=":
    FNR(F(N,R))
1100 NEXT R
1110 NEXT N
1120 FOR T1=1 TO 241 STEP 1
1121 T=(T1-1)/10
1140 FOR N=1 TO 4
1150 K(N)=F(N,1)*SIN(15*N*(T-F(N
    ,2))+90)
1160 NEXT N
1170 H4(T1)=K(1)+K(2)+K(3)+K(4)
1171 DISP C$:"("T")=":FNR(H4(T
    1)): "GAMMAS"
1180 NEXT T1
1181 BEEP
1182 PRINT "" @ PRINT "" @ PRINT
    ""
1190 FOR T=1 TO 24
1191 T1=10*T+1
1200 PRINT C$:"("T")=":FNR(H4(
    T1)): "GAMMAS"
1210 NEXT T
1211 PRINT "" @ PRINT ""
1212 PRINT C$:" "N$:" " "Day"
    :D:"Month":M
1213 PRINT "          AMPLITUDE (G
    ammas)"
1214 PRINT "-20      -10      0
    10      20"
1220 PEN 1 @ GCLEAR ! START GRAP
    H105 SCALE
1230 Y1=-20 ! BOTTOM SCALE SET
1240 Y2=20 ! TOP SCALE SET
1250 SCALE 0,24,Y1,Y2
1260 XAXIS Y1,1,0,24 @ XAXIS Y2,
    1,0,24
1270 XAXIS (Y1+Y2)/2,0 @ XAXIS (
    Y1+Y2)/2+10,0 @ XAXIS (Y1+Y
    2)/2-10,0
1280 YAXIS 0,2,Y1,Y2 @ YAXIS 24,
    2,Y1,Y2
1290 FOR X=1 TO 3

```

EXAMPLE →

```

1300 YAVIS 6*X:0.Y1.Y2
1310 NEXT X:1 END SCALE SET
1311 PENUP
1312 Z=0
1320 FOR T1=1 TO 241 STEP 1
1330 X=(T1-1)/10 @ Y=H4(T1)
1340 IF Y<20 AND Y>=-20 THEN 13
96
1341 IF Y>20 THEN 1343
1342 IF Y<-20 THEN 1356
1343 IF Z=0 THEN 1345
1344 GOTO 1350
1345 PENUP
1346 Z=1
1350 IF Y>20 AND Y<=60 THEN 1391
1351 IF Z=1 THEN 1354
1352 GOTO 1355
1354 PENUP @ Z=0
1355 GOTO 1390
1356 IF Z=0 THEN 1358
1357 GOTO 1360
1358 PENUP @ Z=1
1360 IF Y<-20 AND Y>=-60 THEN 13
81
1361 IF Z=1 THEN 1363
1362 GOTO 1390
1363 PENUP @ Z=0
1380 PEN 1 @ Y=Y+20 @ GOTO 1400
1381 PEN 1 @ Y=Y+40 @ GOTO 1400
1390 PEN 1 @ Y=Y-80 @ GOTO 1400
1391 PEN 1 @ Y=Y-40 @ GOTO 1400
1396 IF Z=0 THEN 1399
1397 PENUP @ Z=0
1399 PEN 1
1400 PLOT X,Y
1410 NEXT T1
1440 PENUP:1 START LABEL
1450 LDIP 0 @ PEN 1
1451 MOVE 12,18.1
1452 LABEL 0#
1460 MOVE 1,-19.9
1470 LABEL "0"
1480 MOVE 6,1,-19.9
1490 LABEL "6"
1500 MOVE 12,1,-19.9
1510 LABEL "12"
1520 MOVE 18,1,-19.9
1530 LABEL "18"
1540 MOVE 22,8,-19.9
1550 LABEL "24"
1560 COPY @ NEXT A
15 @ DISP "IF WANT NEXT MONTH PR
ESS CONT"
1530 FOR I=1 TO 50
1581 BEEP I#RND+1.50
1582 NEXT I
1590 PAUSE
1600 M1=M1+1 @ M=M+1
1610 GOTO 411
1620 END

```

```

15 DEG GEOMAG
4 37 DEG LATITUDE
270 DEG LONGITUDE
15 DEG GEOMAGNETIC LATITUDE
339 74 DEG GEOMAGNETIC LONG
DAY= 21 MONTH= 3
DAY NUMBER FOR YEAR = 80
UT OF LOCAL MOT = 6

```

```

HC 1 )=-8.32 GAMMAS
HC 2 )=-6.61 GAMMAS
HC 3 )=-7.98 GAMMAS
HC 4 )=-7.14 GAMMAS
HC 5 )=-5.28 GAMMAS
HC 6 )=-4.16 GAMMAS
HC 7 )=- 9 GAMMAS
HC 8 )= 4.64 GAMMAS
HC 9 )= 12.3 GAMMAS
HC 10 )= 20.37 GAMMAS
HC 11 )= 25.57 GAMMAS
HC 12 )= 25.67 GAMMAS
HC 13 )= 20.21 GAMMAS
HC 14 )= 11.39 GAMMAS
HC 15 )= 3.63 GAMMAS
HC 16 )=-3.49 GAMMAS
HC 17 )=-6.48 GAMMAS
HC 18 )=-7.61 GAMMAS
HC 19 )=-8.45 GAMMAS
HC 20 )=-9.66 GAMMAS
HC 21 )=-10.83 GAMMAS
HC 22 )=-11.29 GAMMAS
HC 23 )=-10.87 GAMMAS
HC 24 )=-10.01 GAMMAS

```

H 15 DEG GEOMAG Day/ 21 Month
3

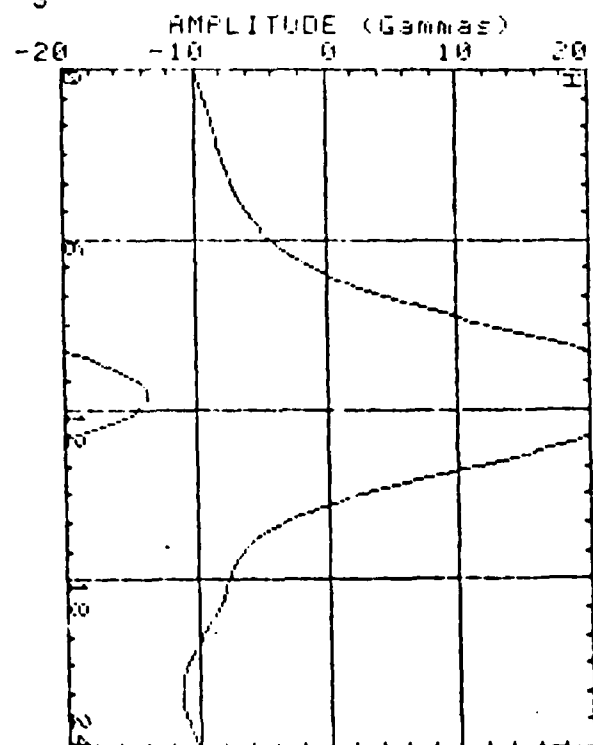


Figure Captions

1. The daily variation in declination $Sq(D)$, the solar zenith angle X , and the Chapman function $\sqrt{\cos X}$ for Honolulu, Hawaii on quiet days in March 1965. The field variation is displayed about its mean position of $11^{\circ}34.56'$ E. Local noon occurs at about 22:32 UT here.
2. The spectral composition of daily variations in declination of Tucson, Arizona for all days of March 1965. a) The spectra between 28 days and 6 hr period; b) The spectra between 6 hr and 5 min period.
3. The monthly average of quiet day field values when $K_p \leq 2+$ in 1965 for the H component of field at Fredericksburg, USA; Huancayo, Peru; and Toolangi, Australia. The scale to the left should be multiplied by 6 to give the Huancayo amplitudes.
4. Difference in appearance of magnetogram H-component values on quiet (21 June 1965, A_p index = 2) and active (15 June 1965, A_p = 19) days. Station letter codes are given to left with the corresponding geomagnetic latitudes. Note the change in amplitude scales for the station values.
5. Results of a superposed-epoch analysis of March, 1965, Honolulu declination variation residuals in lunar time as described in the text. Note the large semidiurnal variation of the lunar tidal component L. 0000 lunar time corresponded to 0450 UT on March 3, 1965. Zero on the amplitude scale corresponds to $11^{\circ}34.56'$ East declination.
6. Comparison of computed lunar field component to the magnetogram record of Honolulu declination (D) component of field on March 20, 1965. Zero on the amplitude scale corresponds to $11^{\circ}34.56'$ East.
7. Variation of Chapman factor with geographic latitude and season. Dashed lines represent Tropic of Cancer and Arctic Circle.

8. Daily variation in Universal Time of solar zenith angle (solid curves) and Chapman factor (dashed curves) for summer solstice (SS), equinox (E), and winter solstice (WS) at Boulder, Colorado.
9. Zonal mean meridional circulation in the earth's thermosphere during equinox and solstice for three levels of auroral activity (Roble, 1981).
10. Magnetospheric contours of ΔB the variation of the observed field from a main field model, in the geomagnetic noon-midnight meridian plane in quiet conditions (Sugira et al., 1971).
11. Seasonal variation of midnight levels of H, D, and Z field components for 5° increments from the equator to 30° geomagnetic latitude (Campbell, 1981).
12. Block diagrams of the contributors to ionosphere current and its surface observation. a) general diagram, b) details of upper part of general diagram, c) details of lower part of general diagram.
13. Values for annual mean phase in hour of first amplitude maximum, for 12-hr component of Sq(H). Point values are indicated with the associated station codes (Table 1) and line segments connecting these values. Smooth curve is obtained from 5-point smoothing of values read from line segments at 2.5° intervals with natural extensions for the curve ends.
14. Daily variation of Sq in 5° geomagnetic latitude increments for March, June, September and December. Scale to right indicates 20 gammas between rows. a) Sq(H); b) Sq(D); c) Sq(Z).
15. Annual mean values of Sq in 5° geomagnetic latitude increments for H, D, and Z. Scale to right indicates 25 gammas between rows.

16. Annual and semiannual amplitude variations of Sq for the separated 24-, 12-, 8-, and 6-hr component periods. Representative plots at 0° , 30° , 60° , 75° , and 90° geomagnetic latitude are shown for the H, D, and Z field directions.
17. Annual and semiannual variation in 24-hr component amplitude of Sq for 5° geomagnetic latitude increments. Scale to right indicates 5 gammas between rows in the H, D, and Z field direction columns.
18. Annual and semiannual variation in 12-hr component amplitude of Sq for 5° geomagnetic latitude increments. Scale to right indicates 5 gammas between rows in the H, D, and Z field direction columns.
19. Measure of fit of Fourier analysis values (FIT) to station observations (OBS) using hourly values in March, June, September and December, for 15 stations plotted at their respective geomagnetic latitudes. a) (bottom) mean residual (error) values as difference between FIT and OBS; b) (middle) residuals as percent of range of OBS; and c) (top) correlation coefficients between FIT and OBS.
20. Estimated error between Fourier analysis values (FIT) and station observations (OBS) partitioned between the annual mean, annual variation, and semiannual variation in proportion to the respective Fourier component amplitudes. Values for 15 stations plotted at their respective geomagnetic latitudes is illustrated for a) (top) Sq(H), b) (middle) Sq(D), and c) (bottom) Sq(Z).

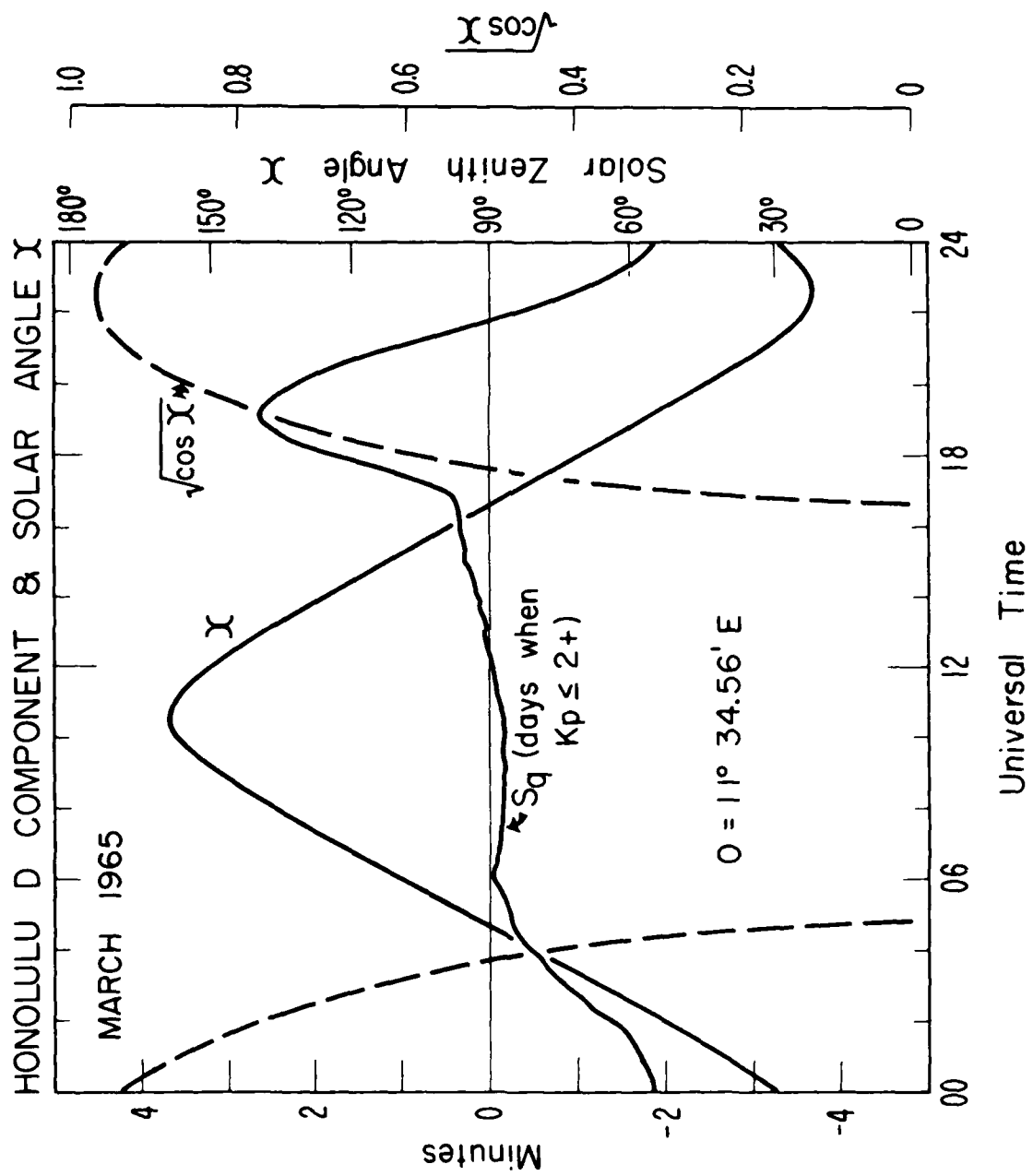


Figure 1

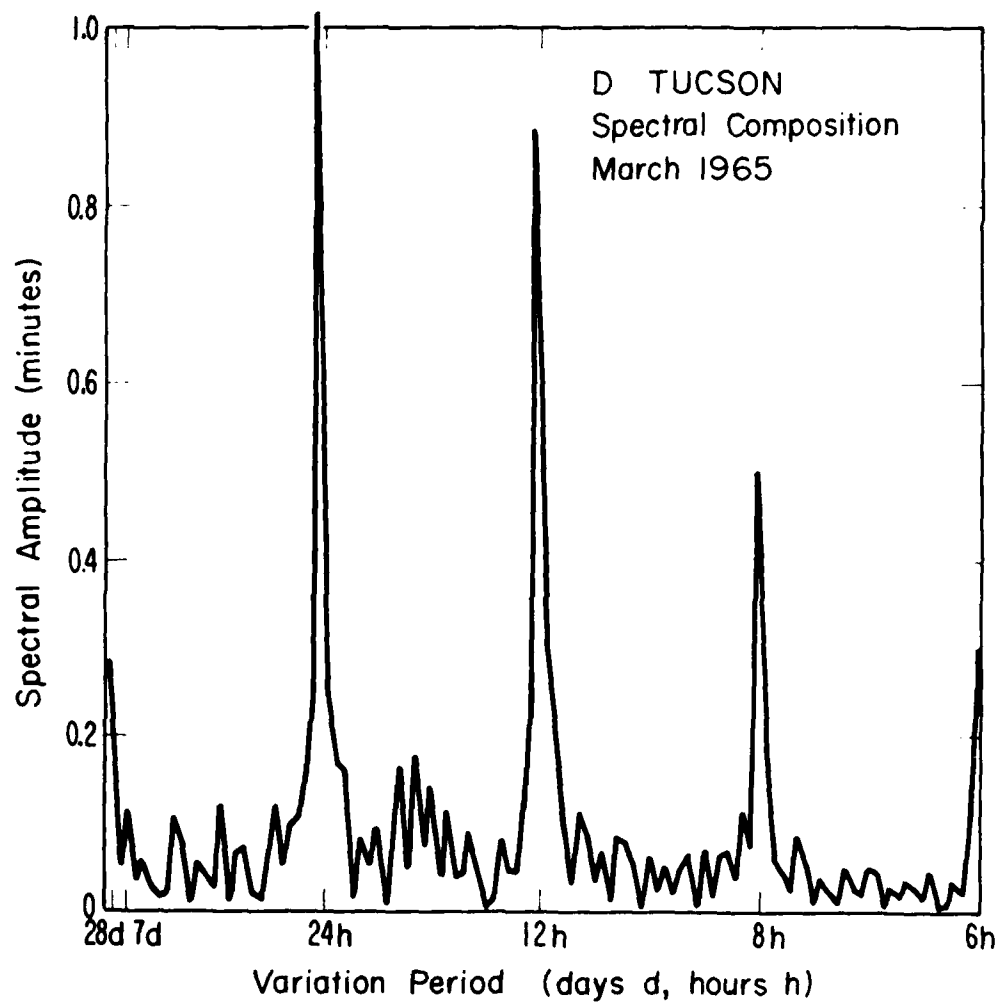


Figure 2a

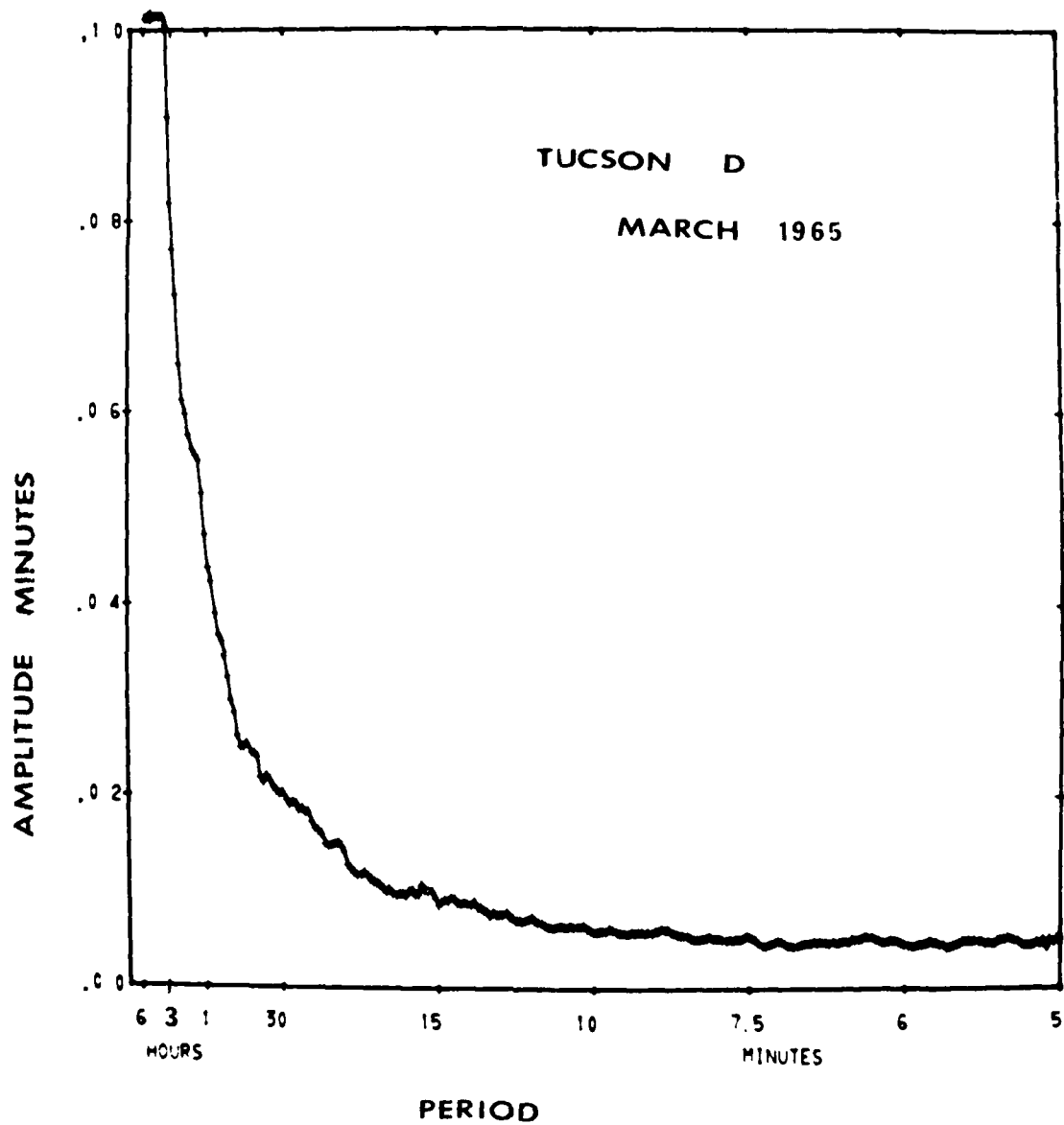
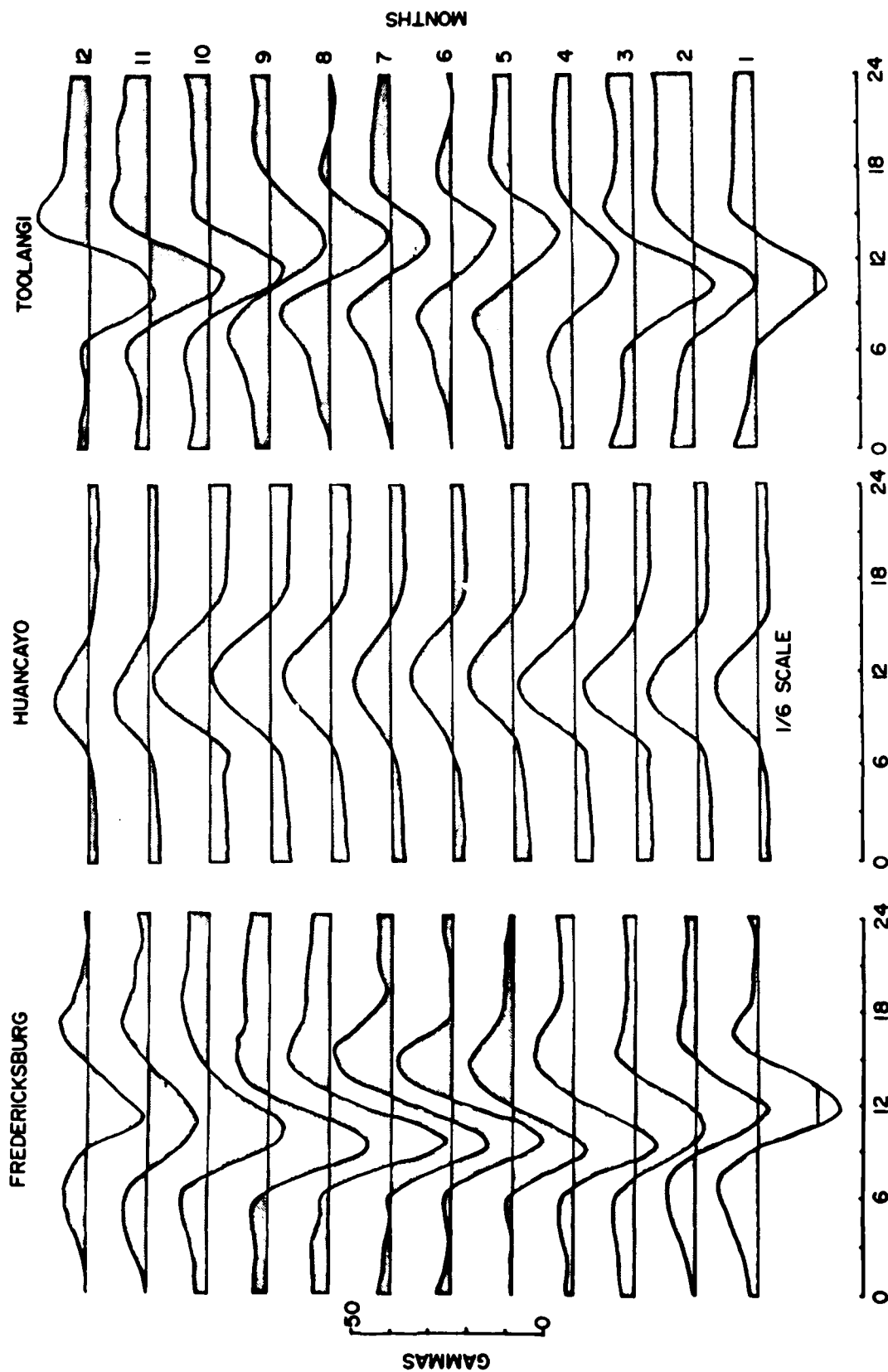


Figure 2b

QUIET SOLAR COMPONENT H



LOCAL MERIDIAN TIME

H
21 JUNE 1965
Ap=2

TH
890°

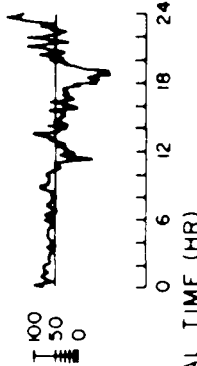
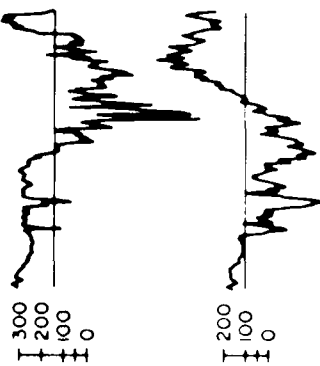
AT
859°

BL
738°

FC
687°

ME
619°

H
15 JUNE 1965
Ap=19



H
21 JUNE 1965
Ap=2

FR
495°

DS
430°

SJ
296°

FO
169°

HU
-06°

GAMMAS

50
30
0

50
30
0

30
0

30
0

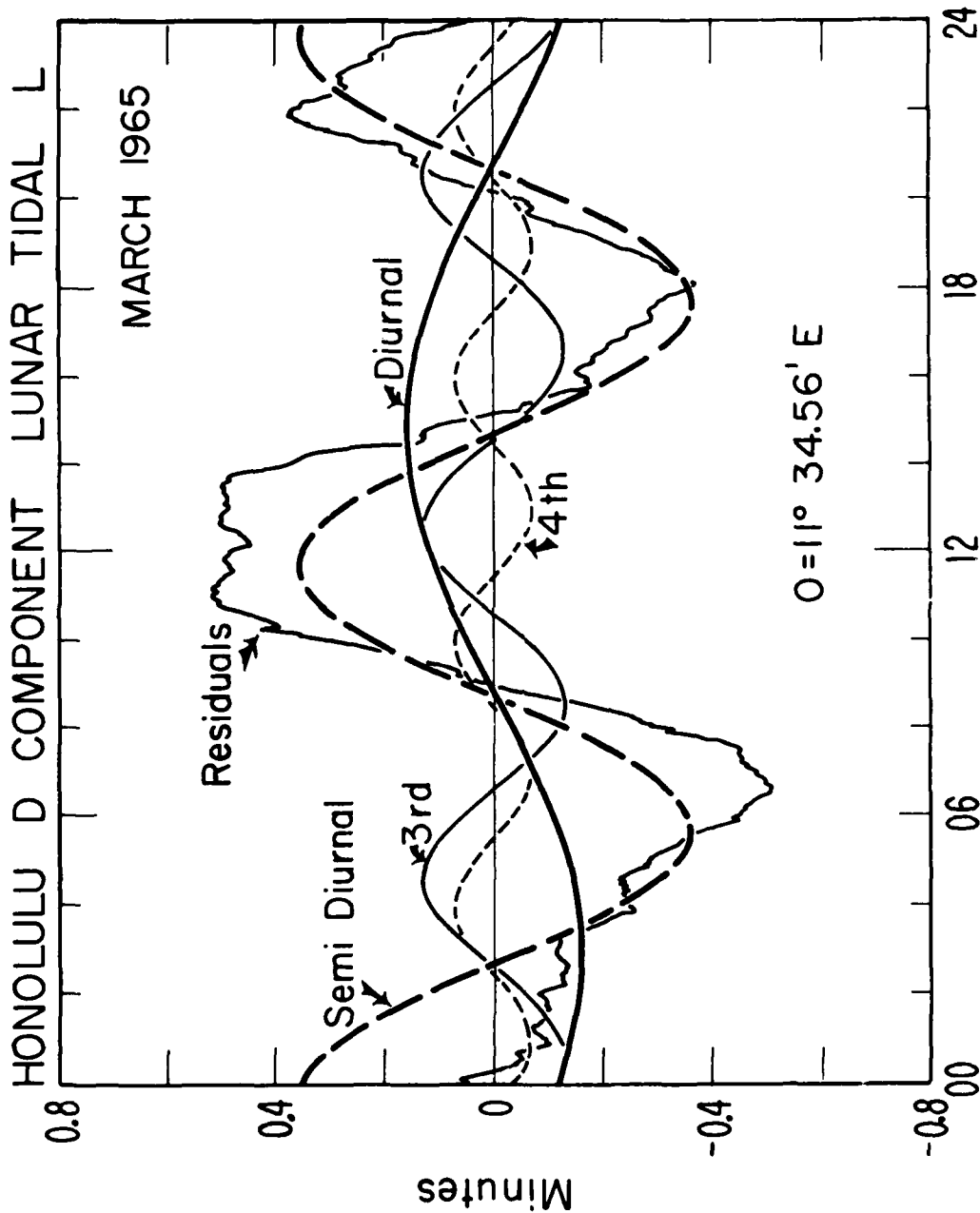
50
30
0

0 6 12 18 24
UNIVERSAL TIME (HR)

H
15 JUNE 1965
Ap=19



0 6 12 18 24
UNIVERSAL TIME (HR)



Lunar Time (0000=0450 UT, March 3)

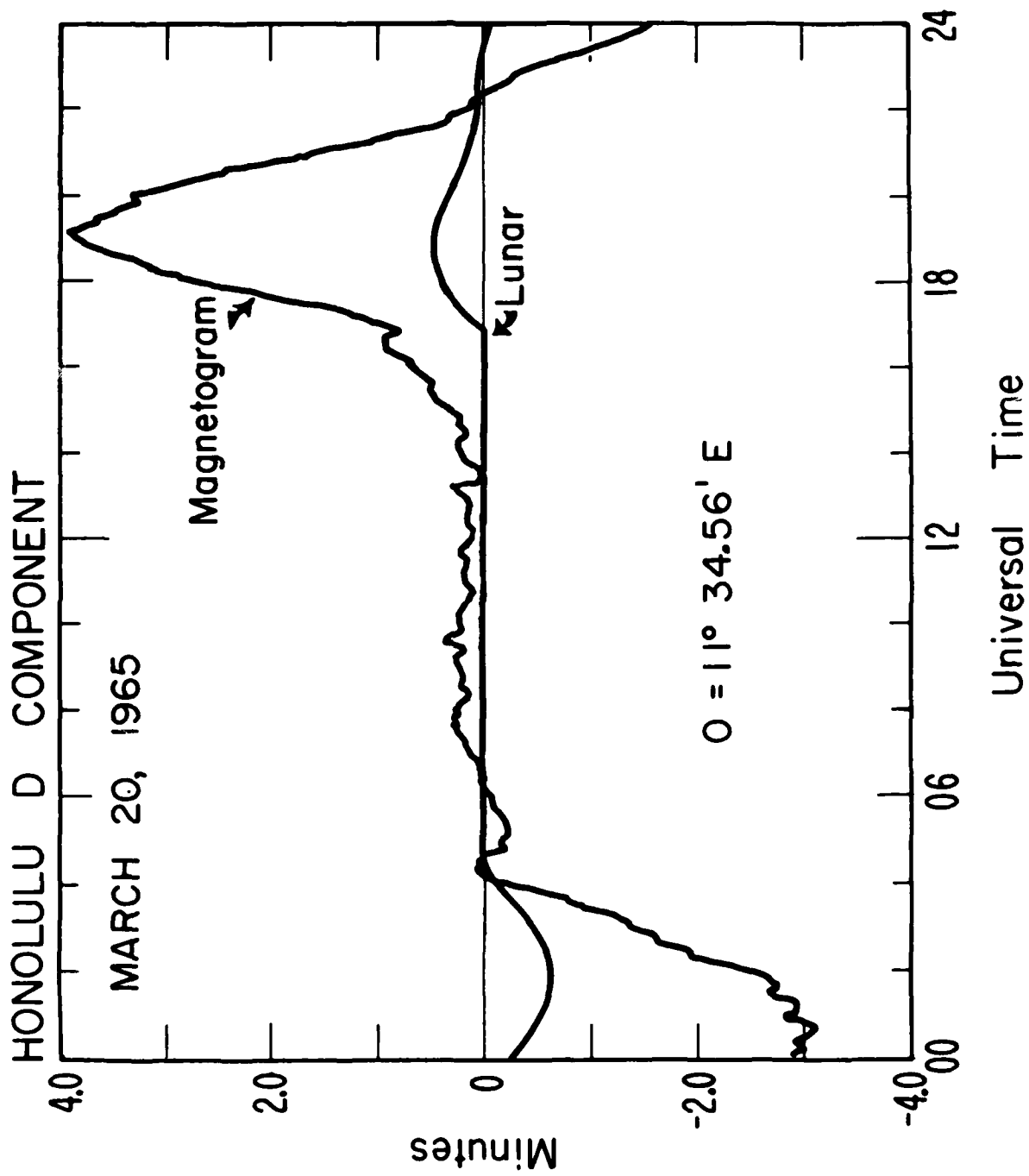


Figure 1

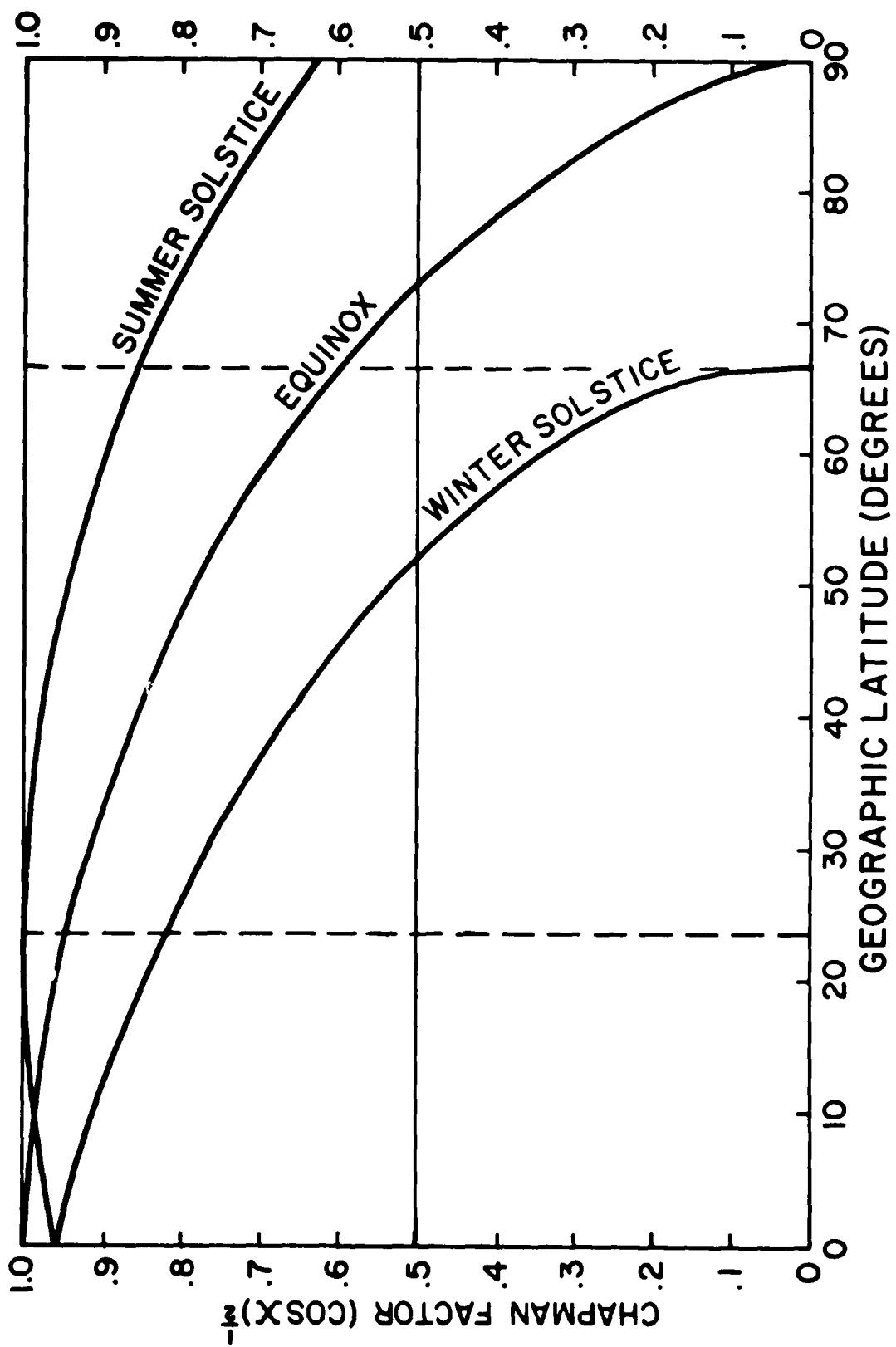


Figure 7

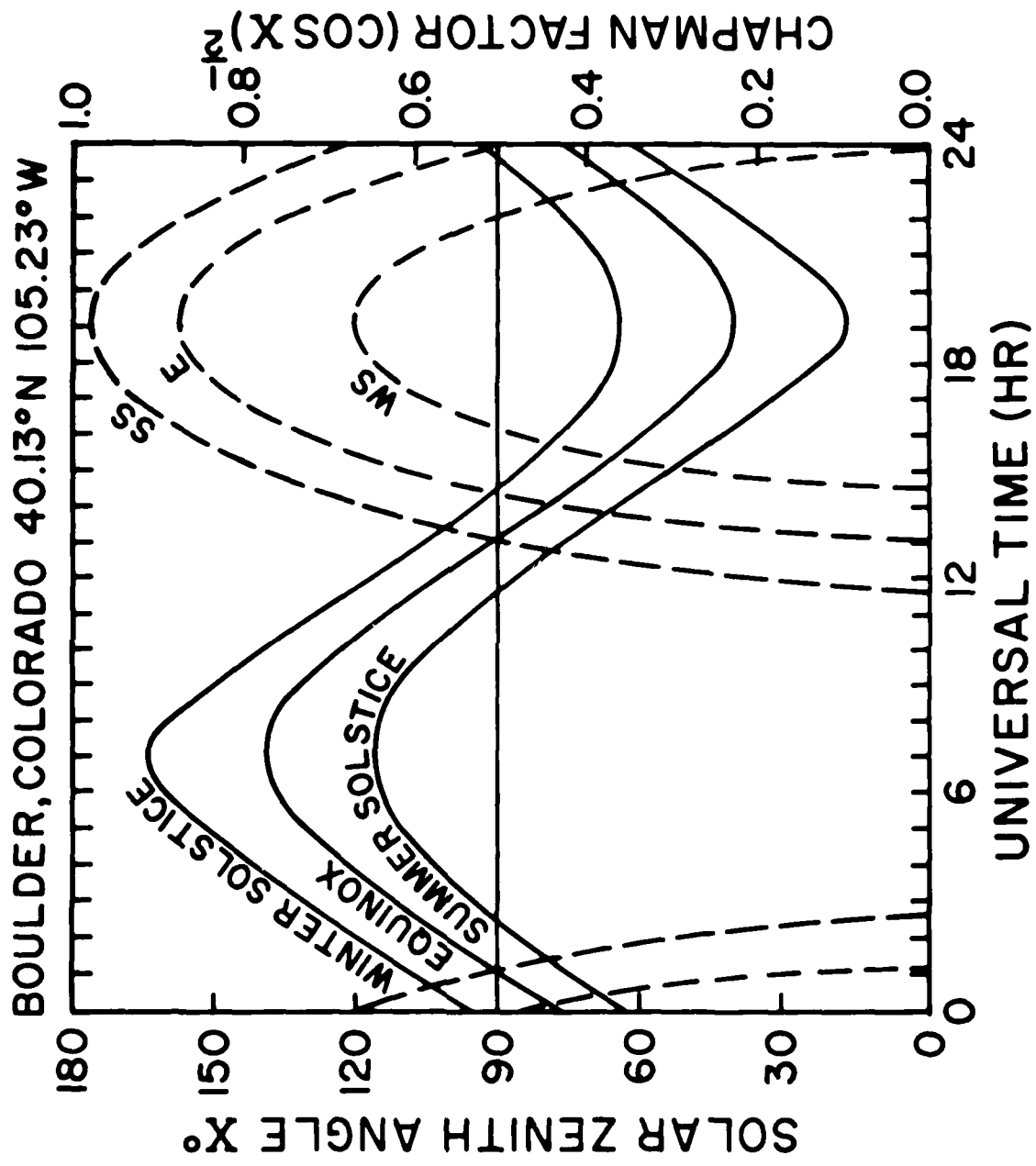
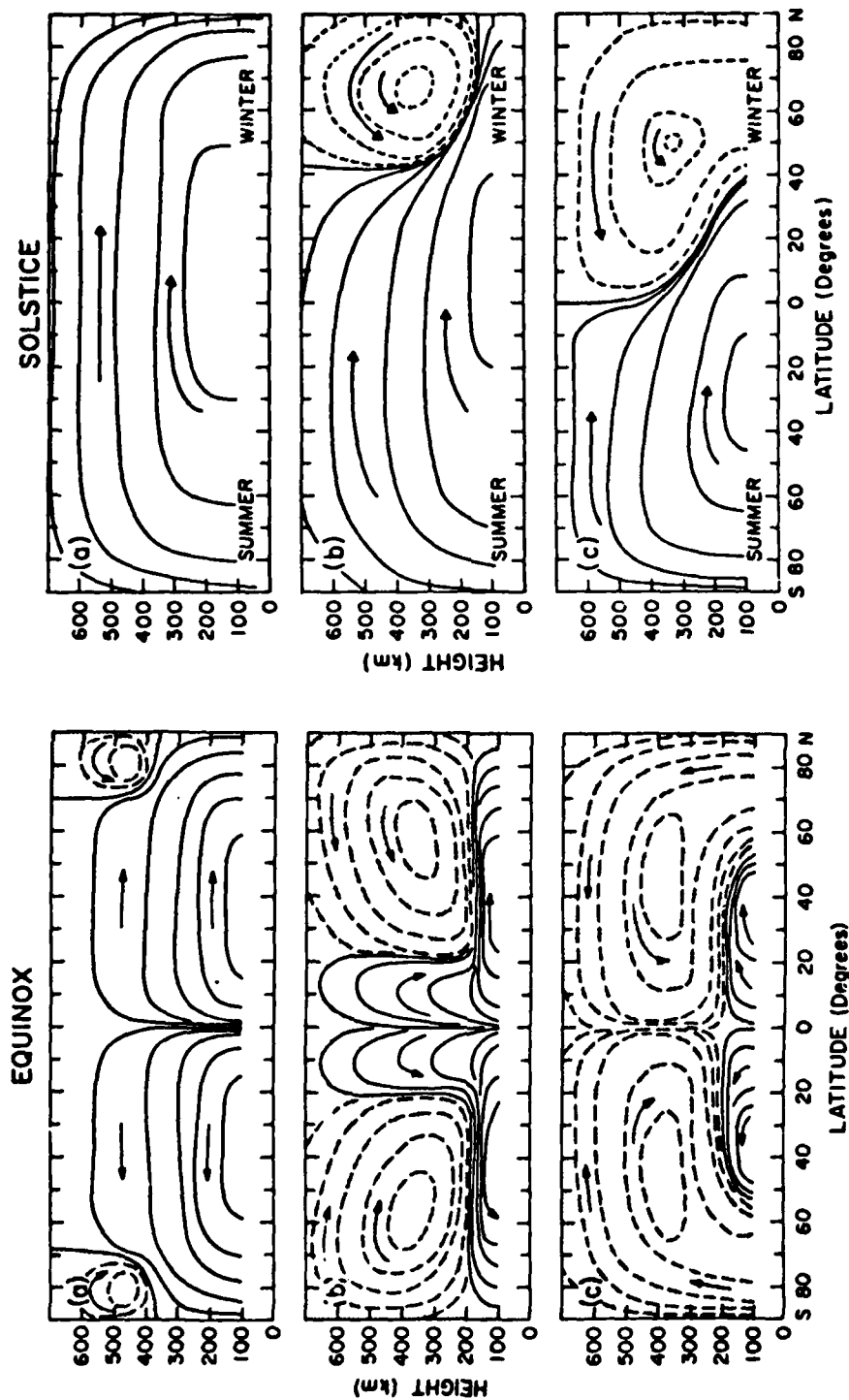


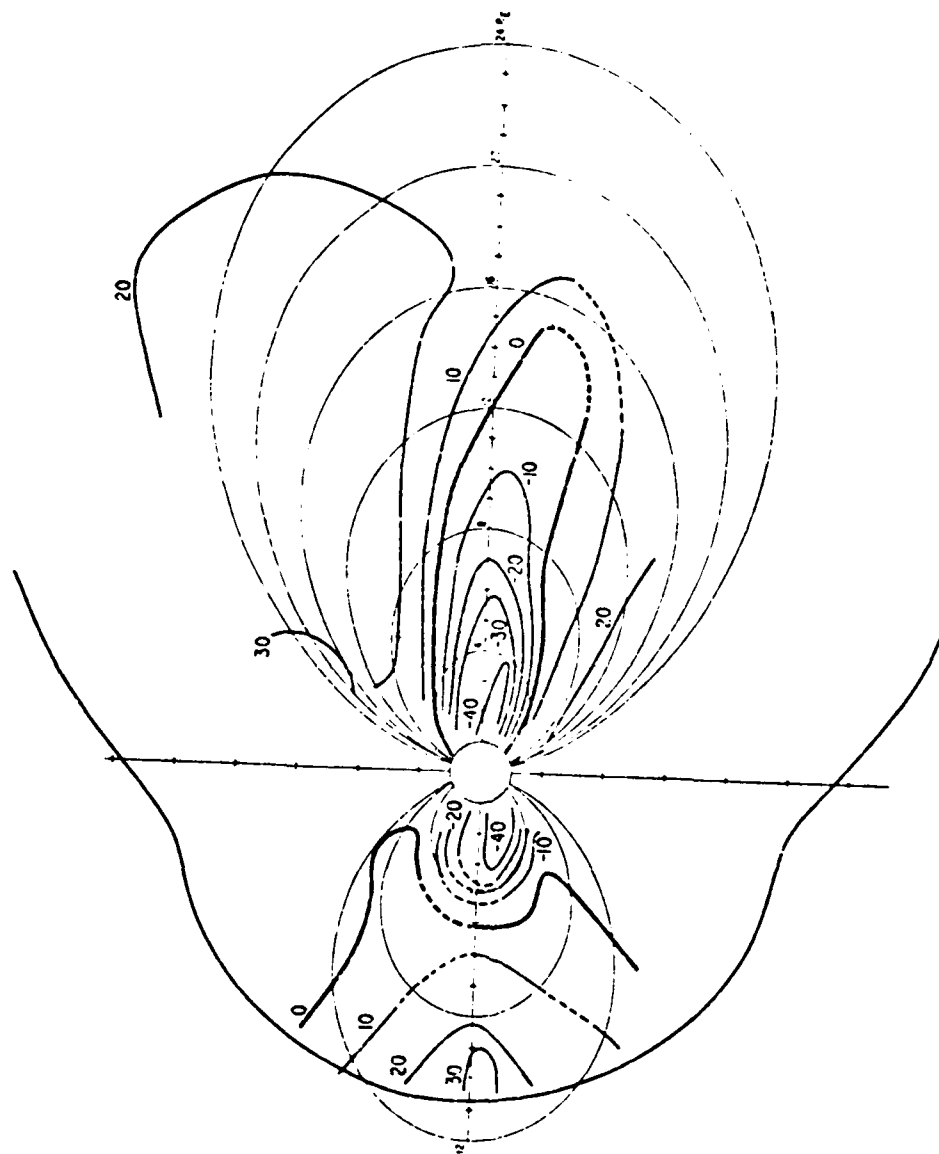
Figure 1



Schematic diagram of the zonal mean meridional circulation in the earth's thermosphere during equinox for various levels of auroral activity: (a) extremely quiet geomagnetic activity, (b) average activity, and (c) geomagnetic substorm. [Source: NCAR]

Schematic diagram of the zonal meridional circulation of the earth's thermosphere during solstice for various levels of auroral activity: (a) extremely quiet geomagnetic activity, (b) average activity, and (c) geomagnetic substorm. [Source: NCAR]

Raymond G. Roble, 1981



Contours of equal ΔB in the geomagnetic noon-midnight meridian plane for a quiet condition, $Kp = 0-1$; units: gammas.

M. SUGIURA, B. G. LEDLEY, T. L. SKILLMAN, AND J. P. HEPPNER 1971

ANNUAL AND SEMIANNUAL AMPLITUDE VARIATION

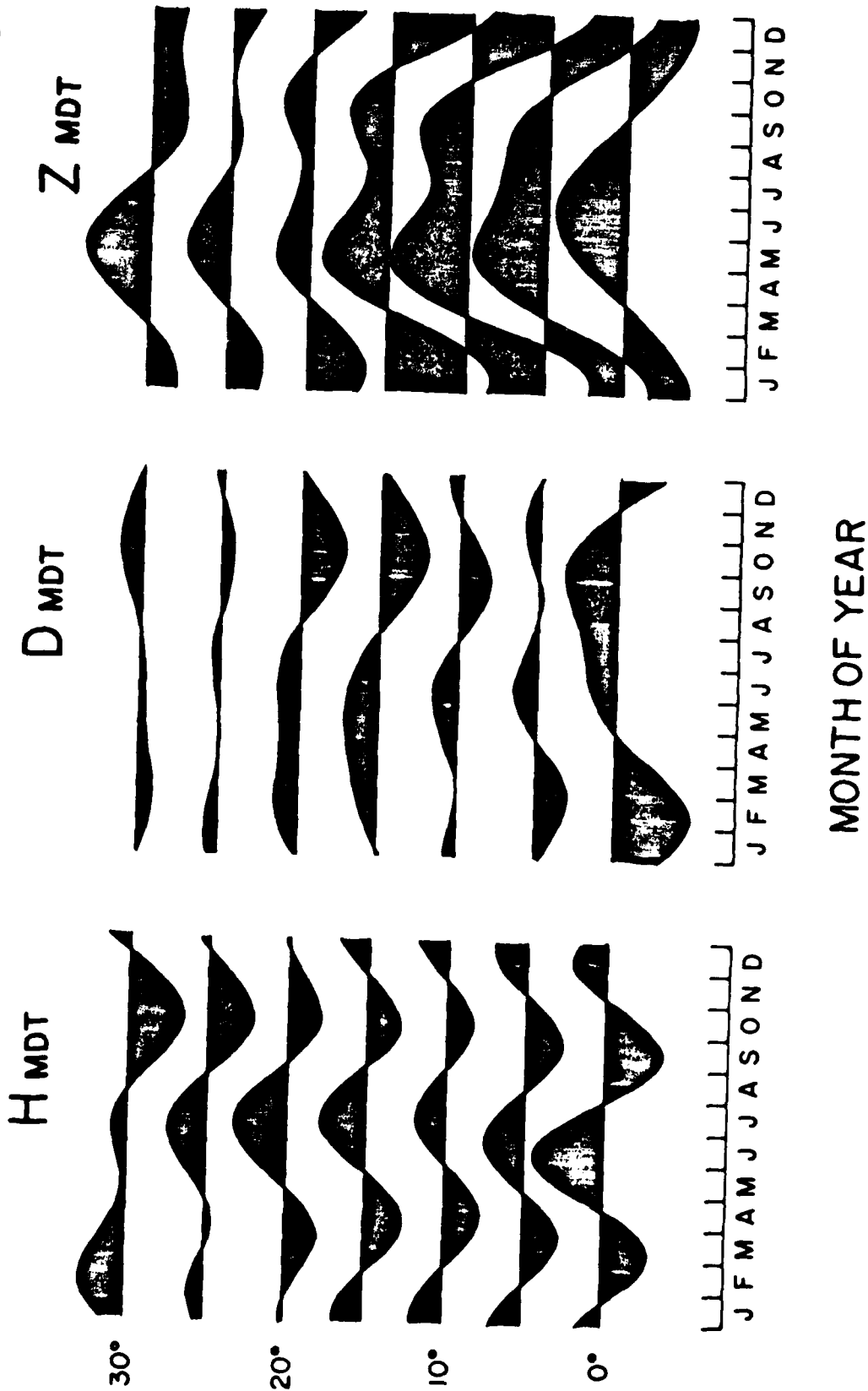


Figure 11

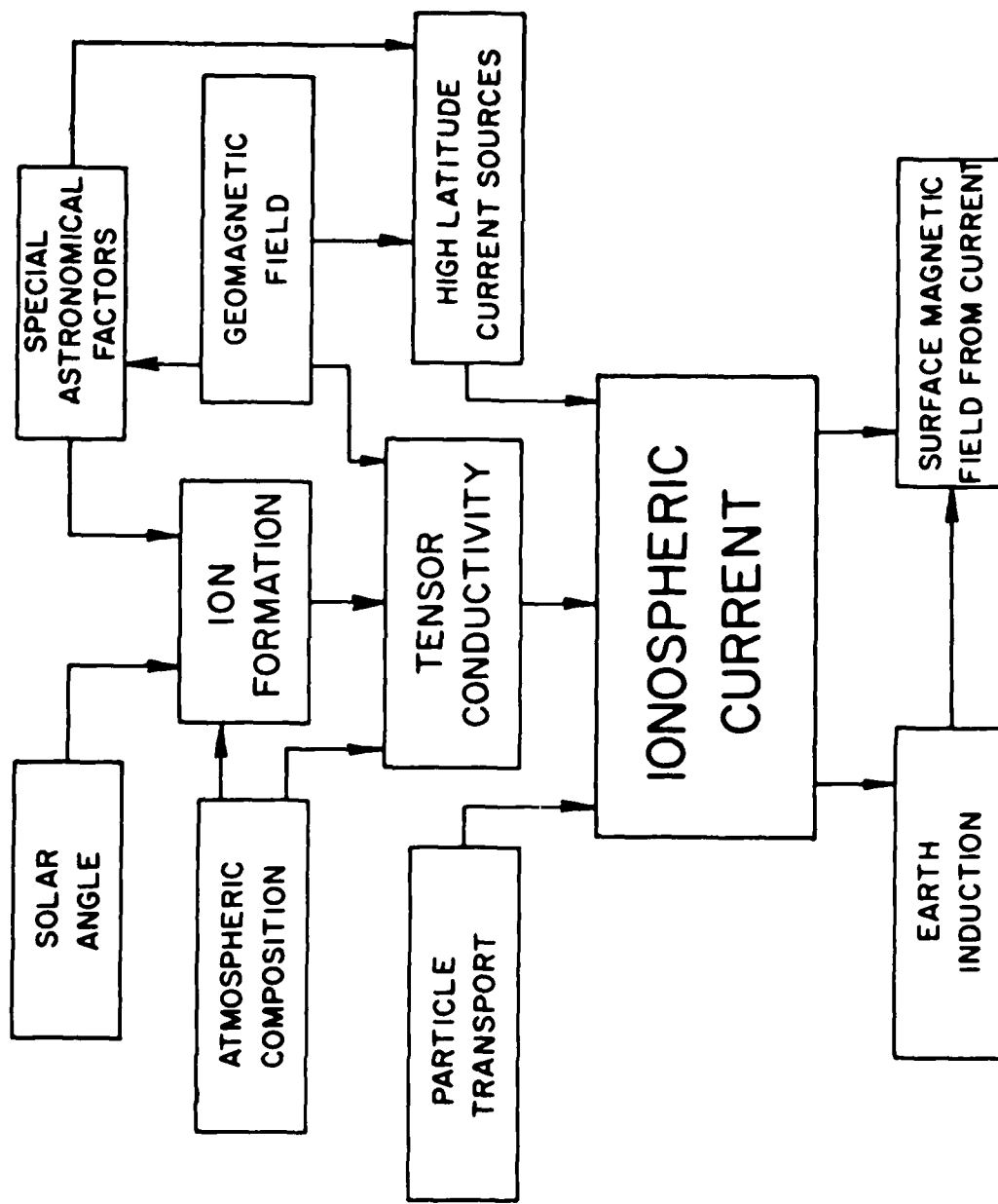


Figure 10

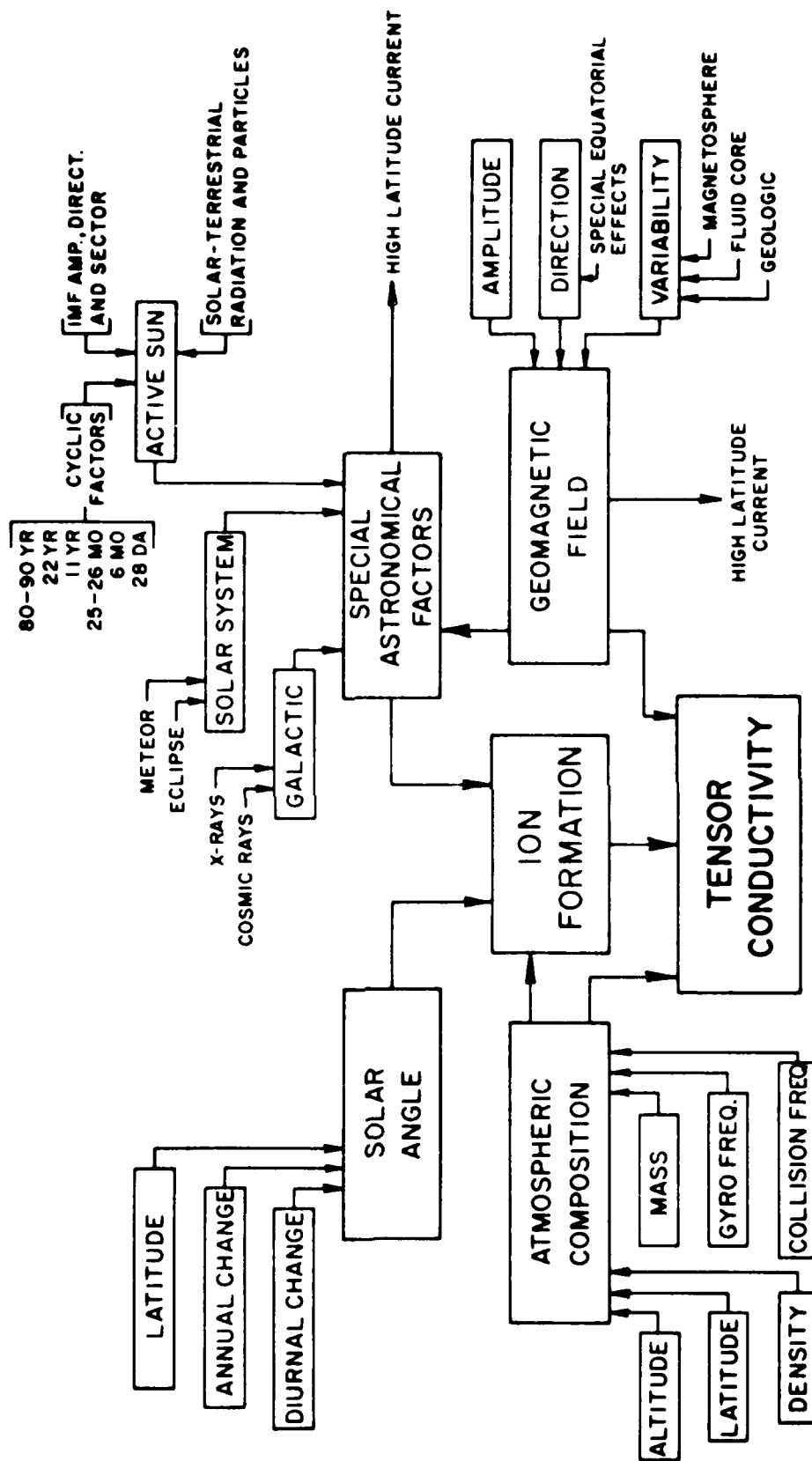


Figure 1-1

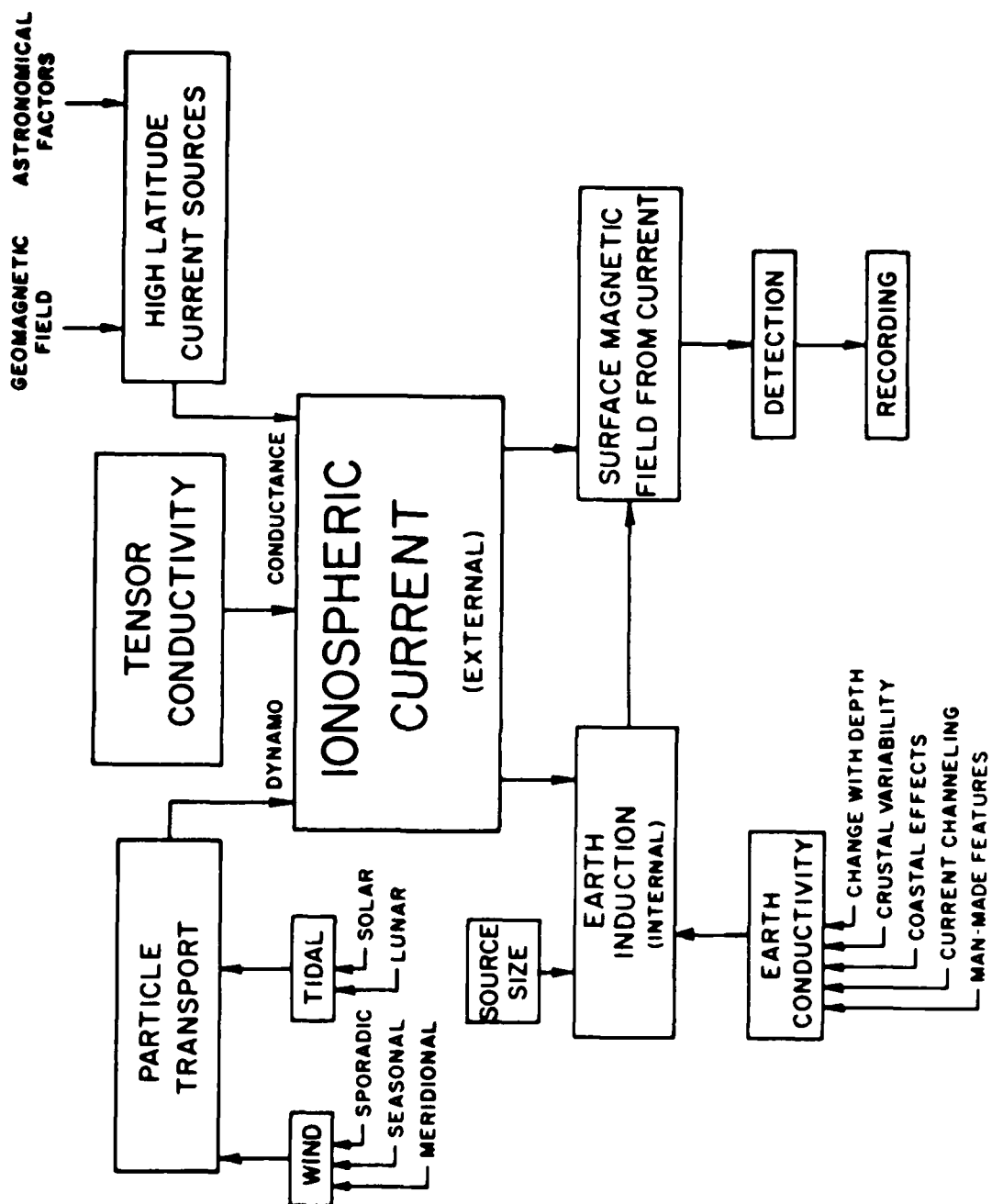
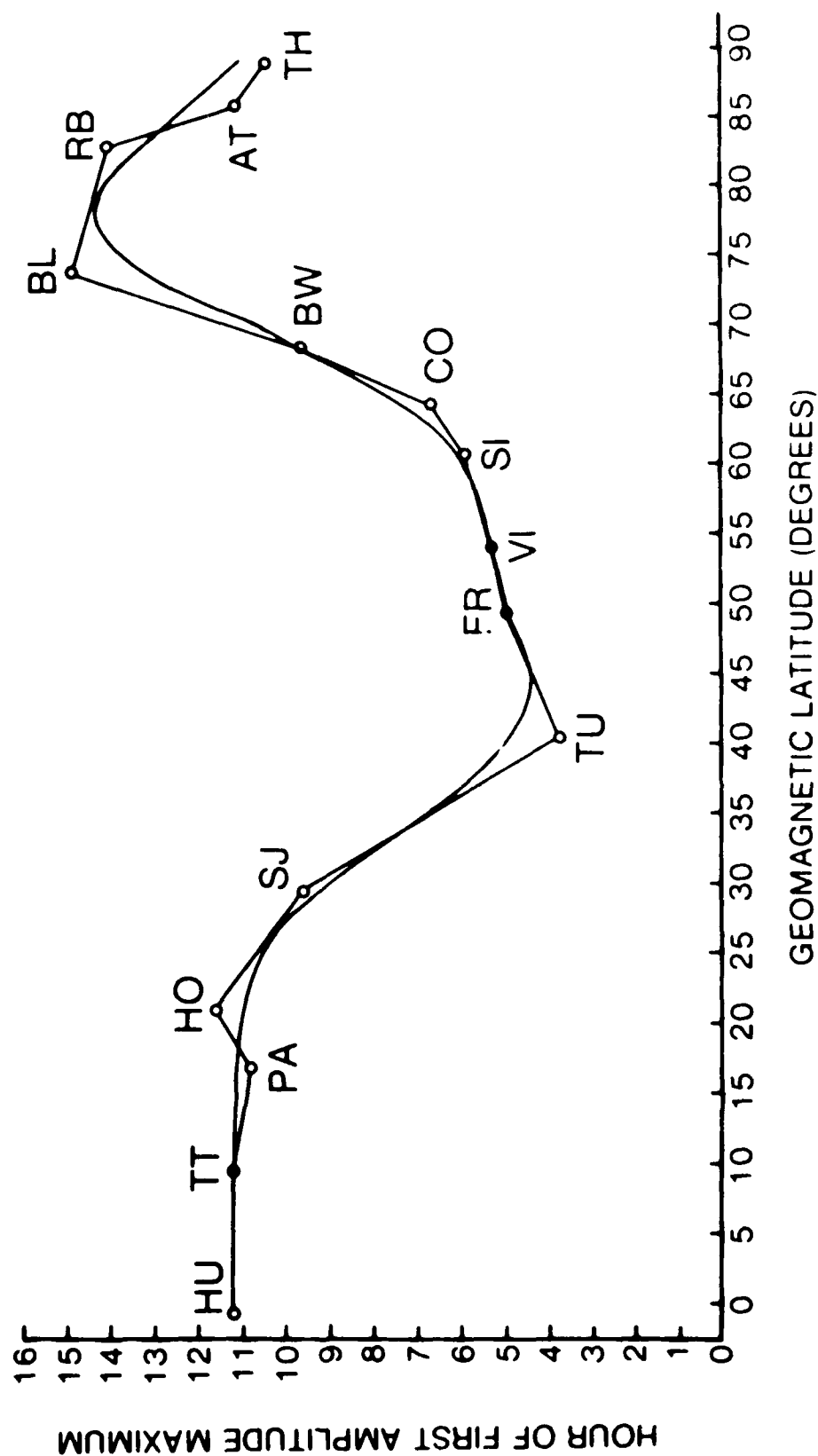


Figure 12

Sq(H) 12-hr COMPONENT ANNUAL MEAN PHASE $\alpha_0/2$



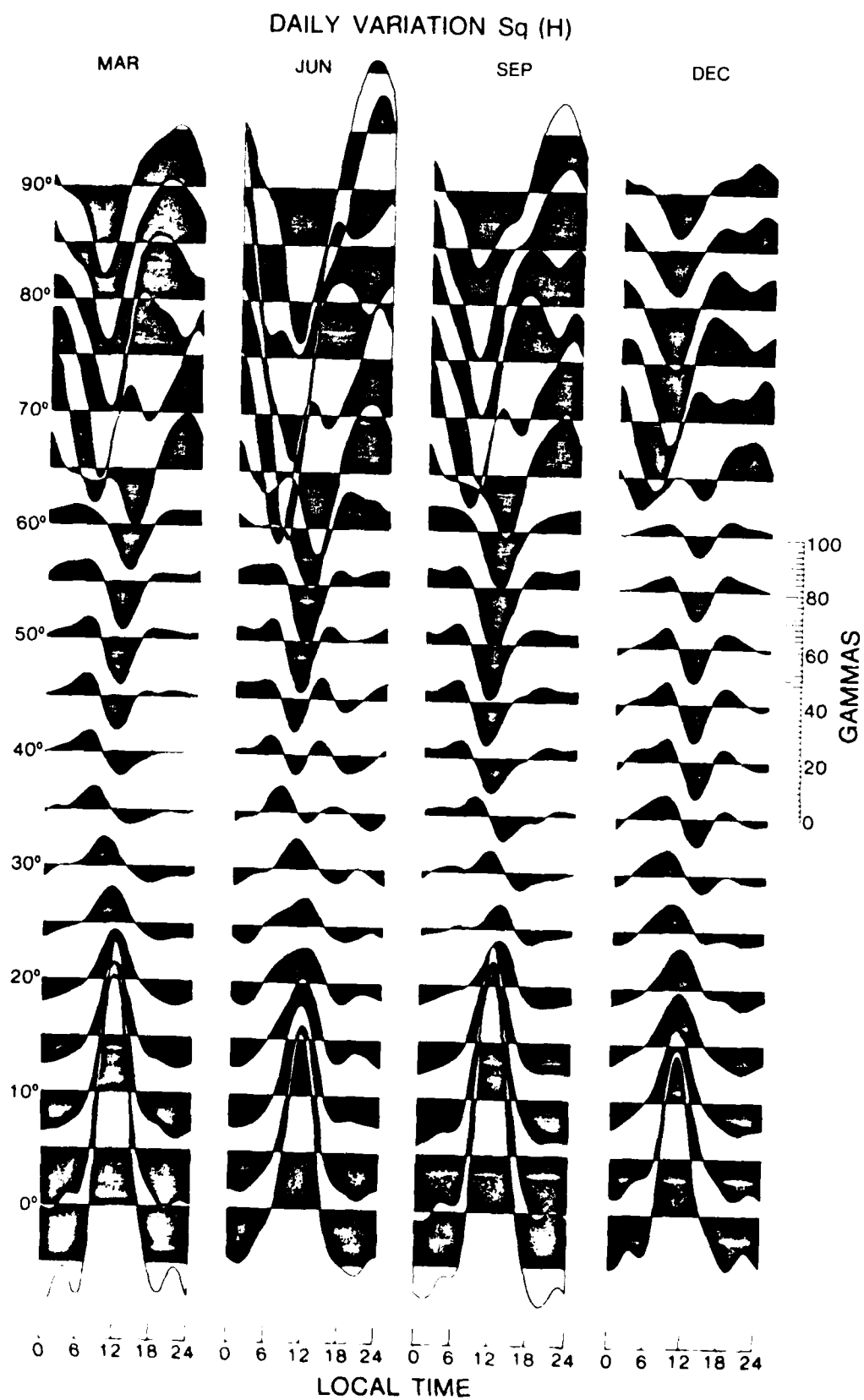


Figure 14a

DAILY VARIATION Sq (D)

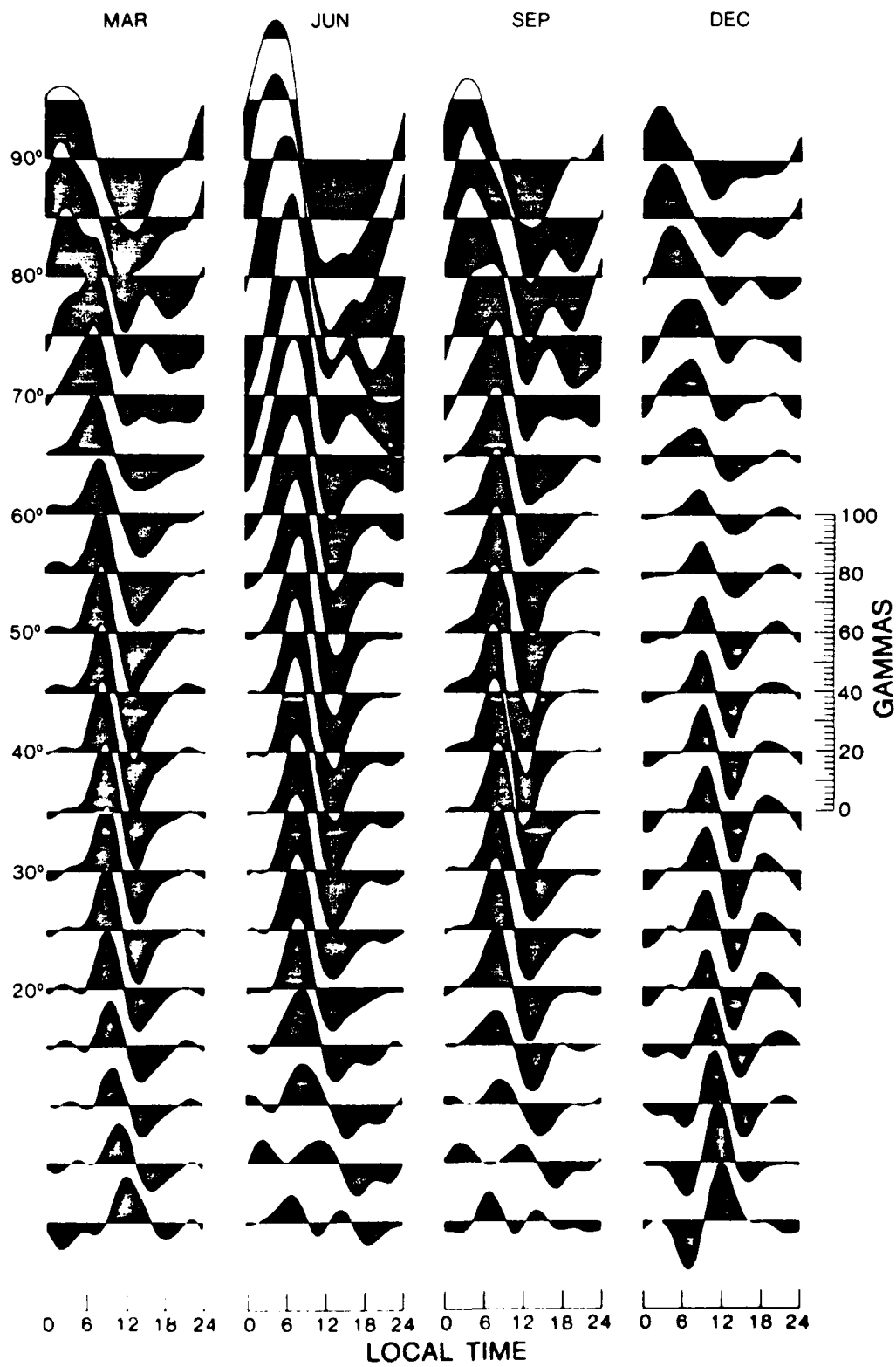
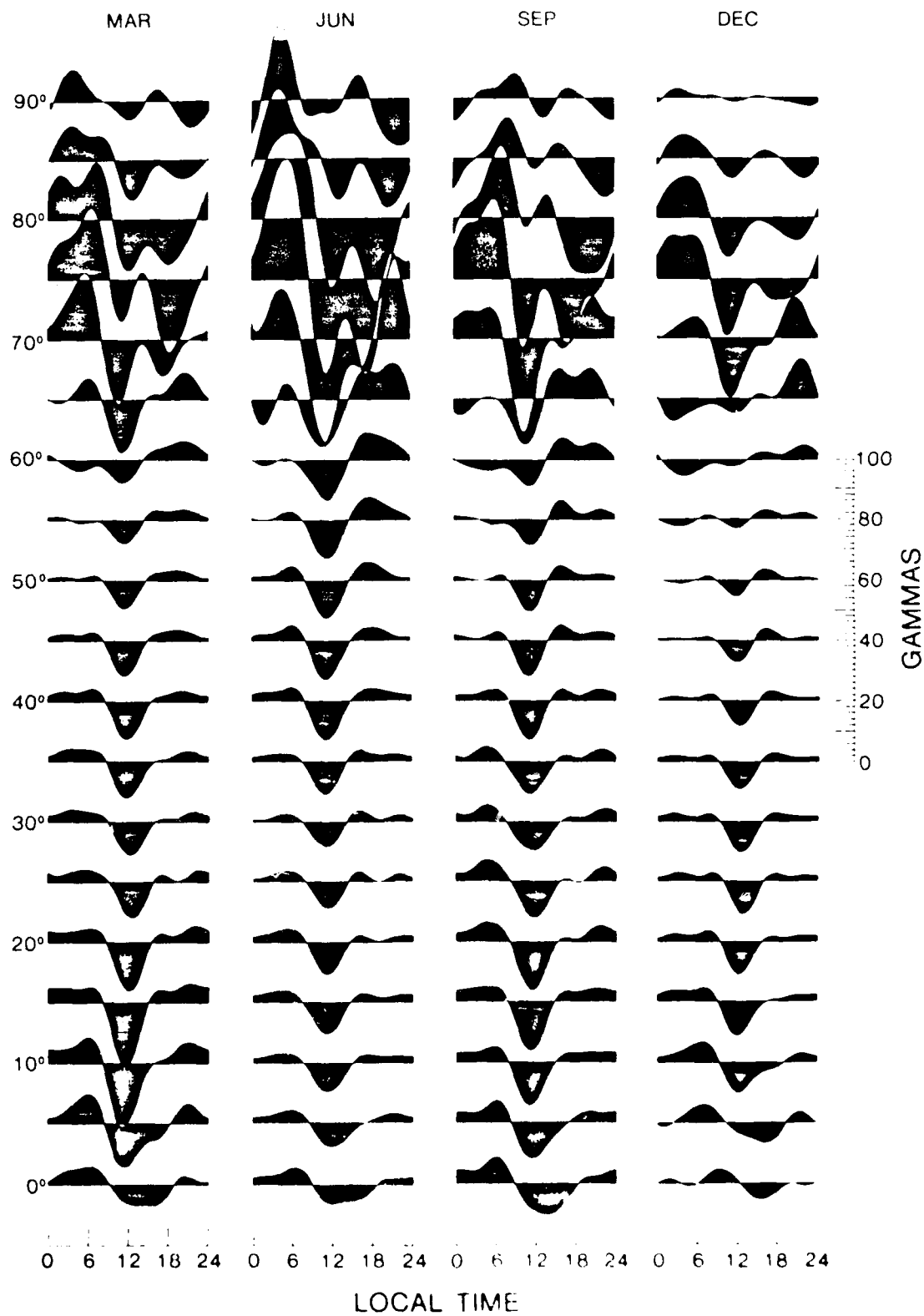


Figure 10

DAILY VARIATION Sq (Z)



ANNUAL MEAN Sq

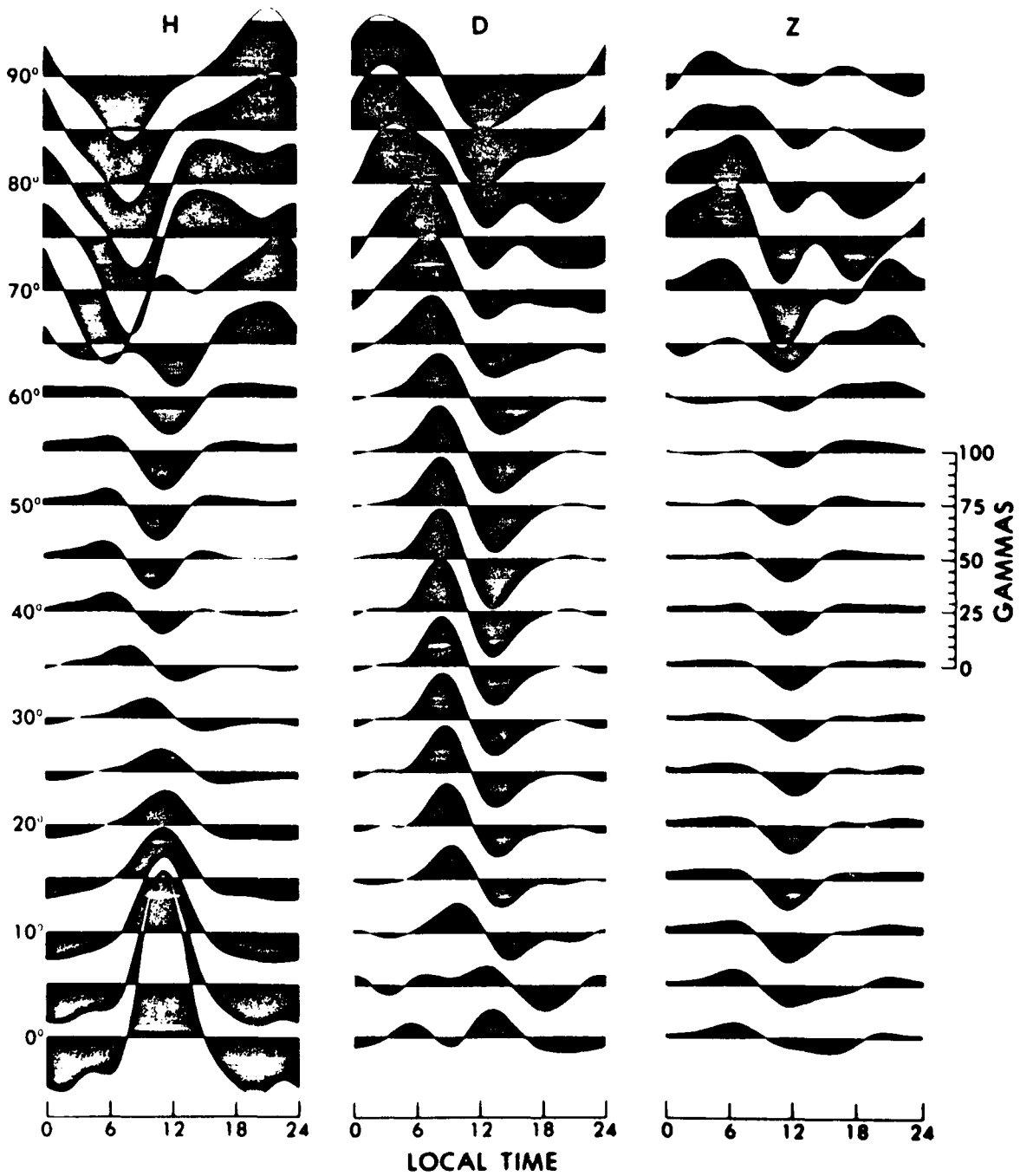


Figure 11

Sq ANNUAL AND SEMIANNUAL AMPLITUDE VARIATIONS

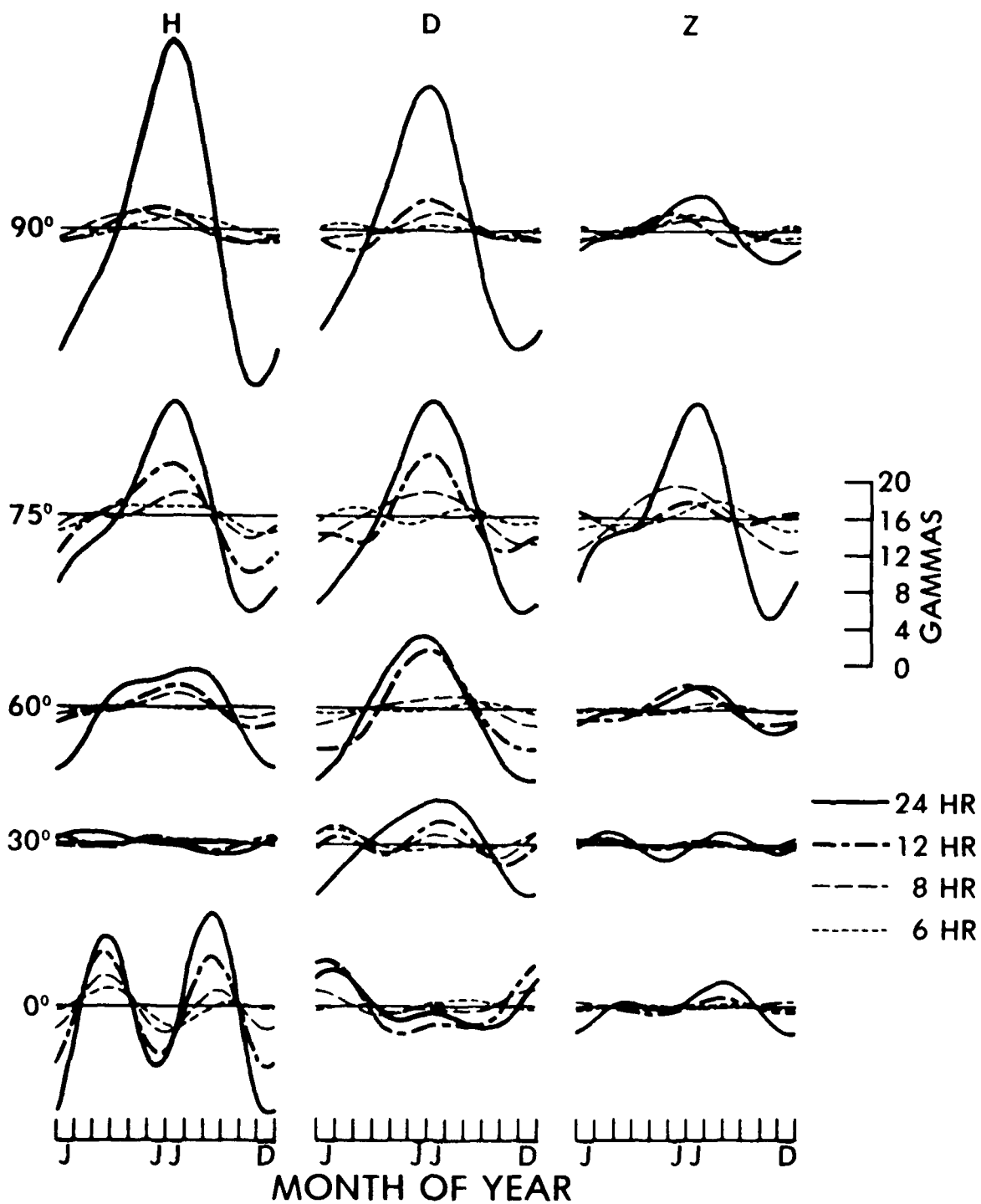


Figure 1

ANNUAL AND SEMIANNUAL VARIATION 24-HR COMPONENT AMPLITUDE OF Sq

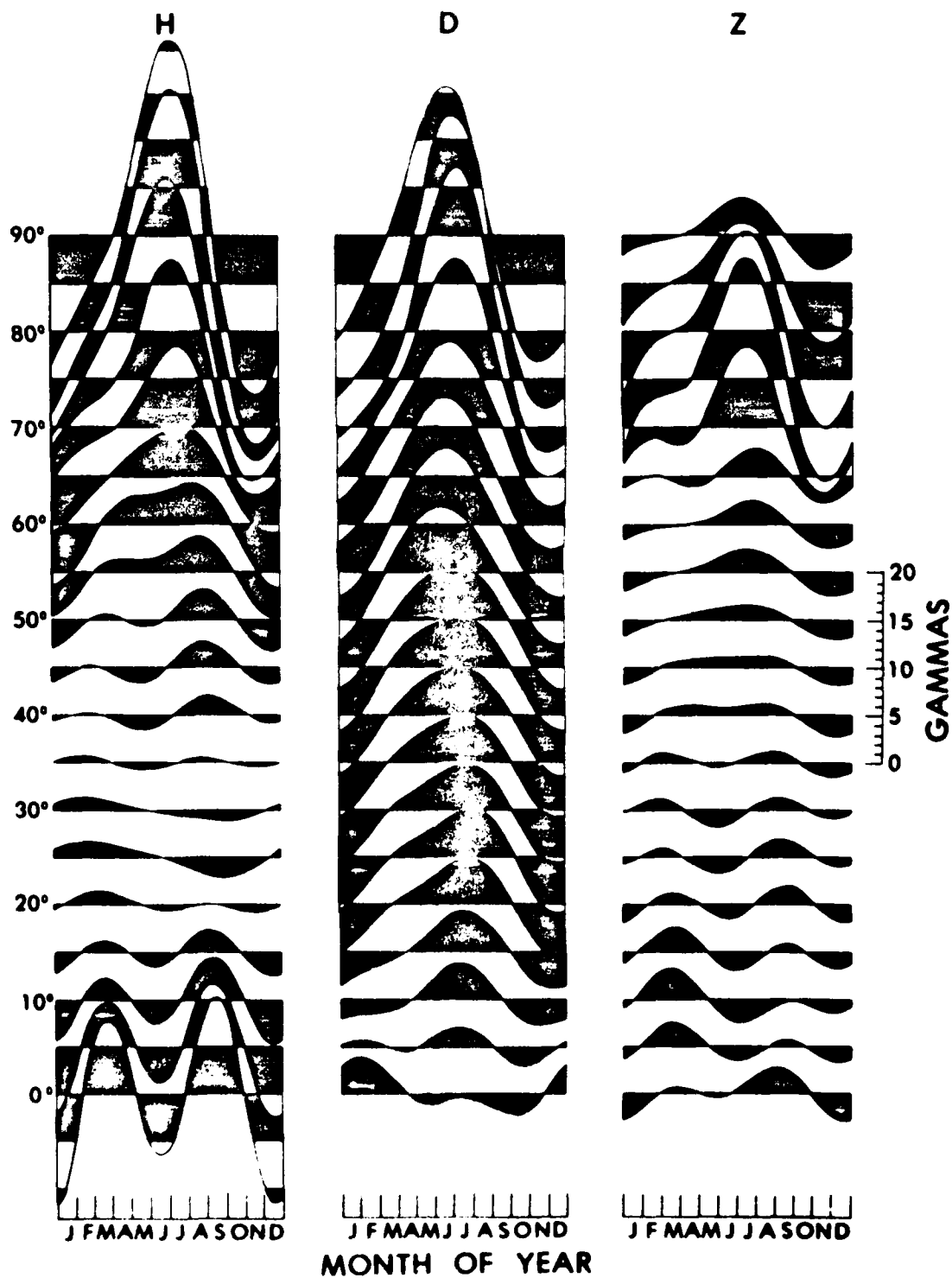
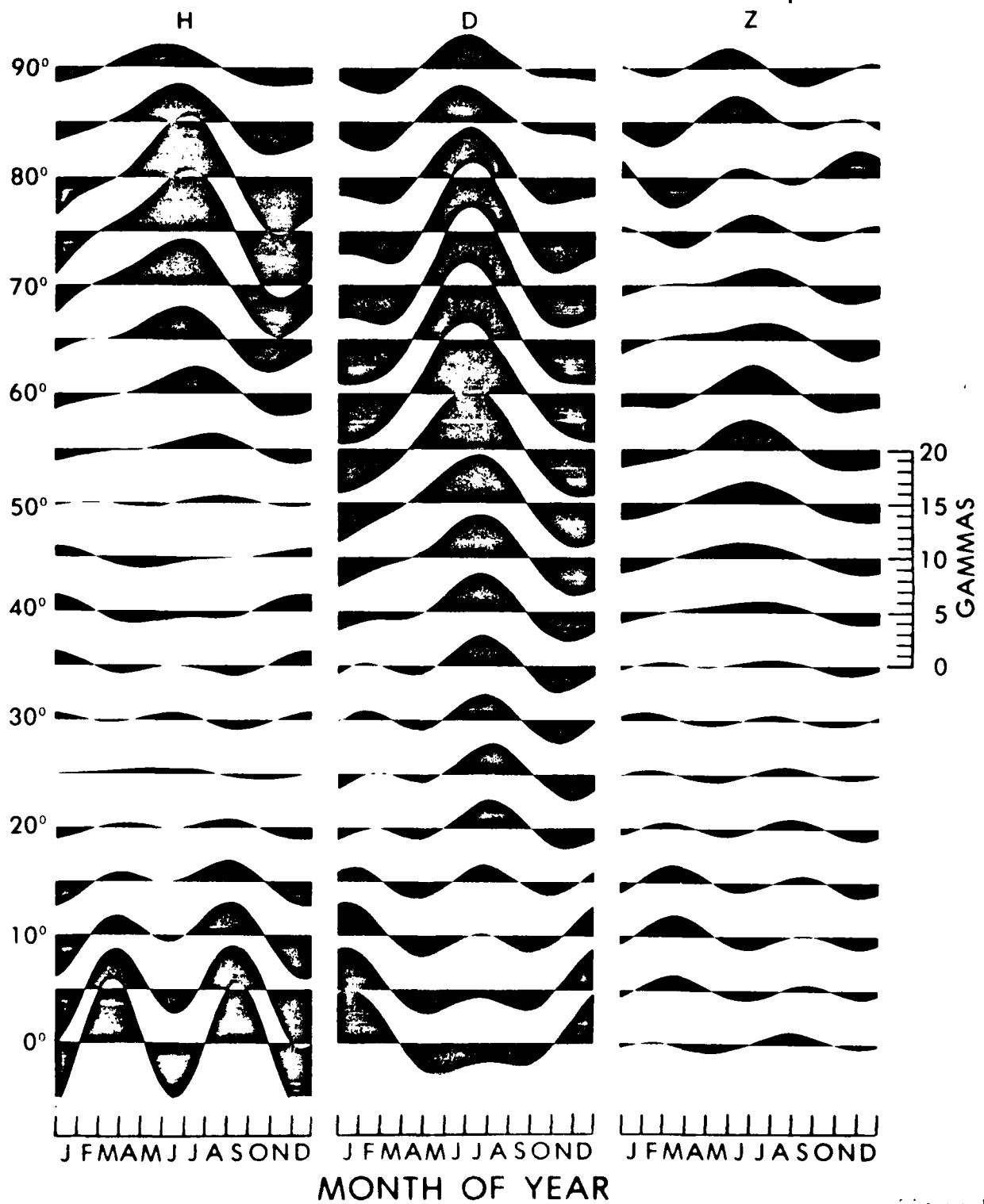


Figure 17

ANNUAL AND SEMIANNUAL VARIATION 12-HR COMPONENT AMPLITUDE OF S_q



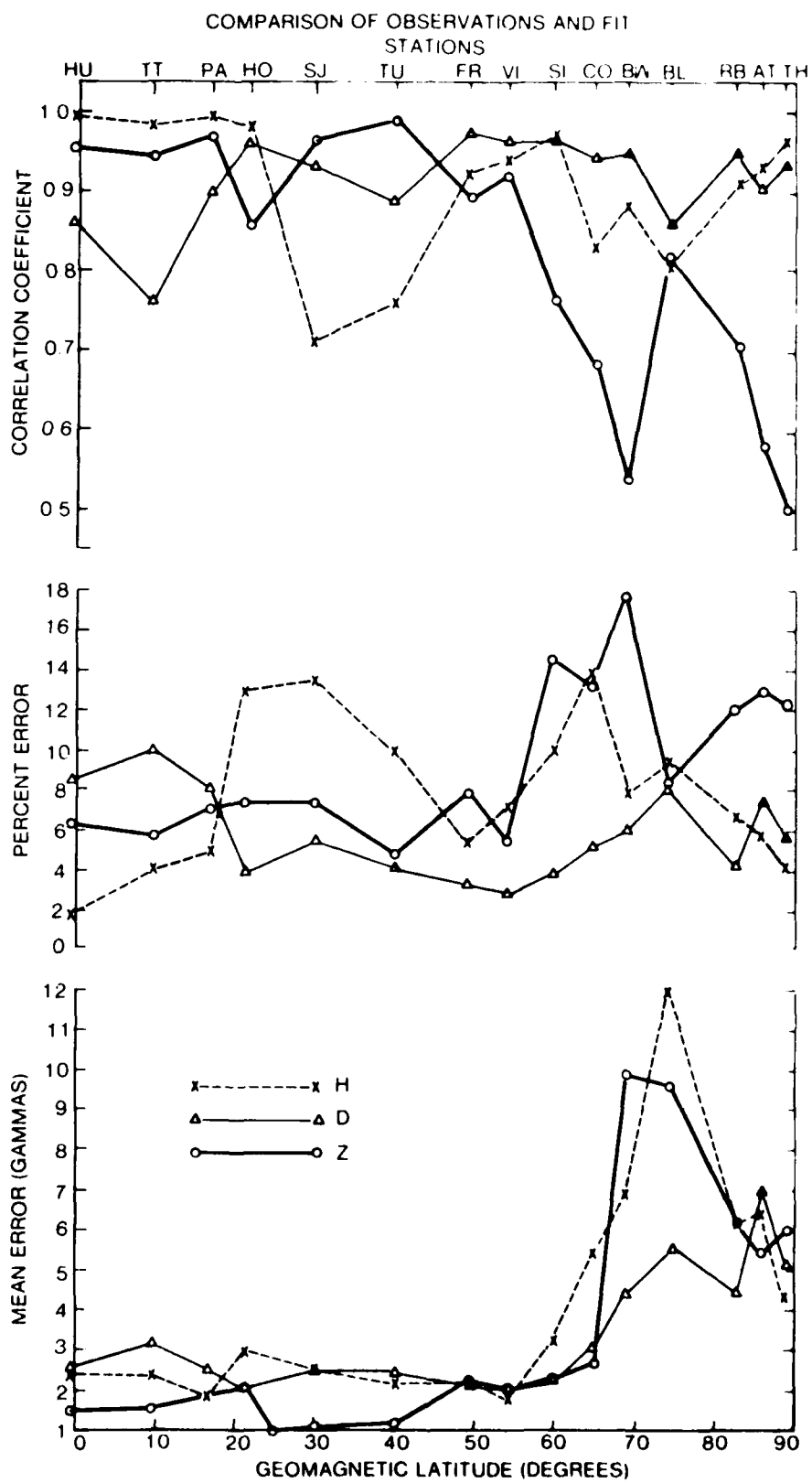


Figure 12

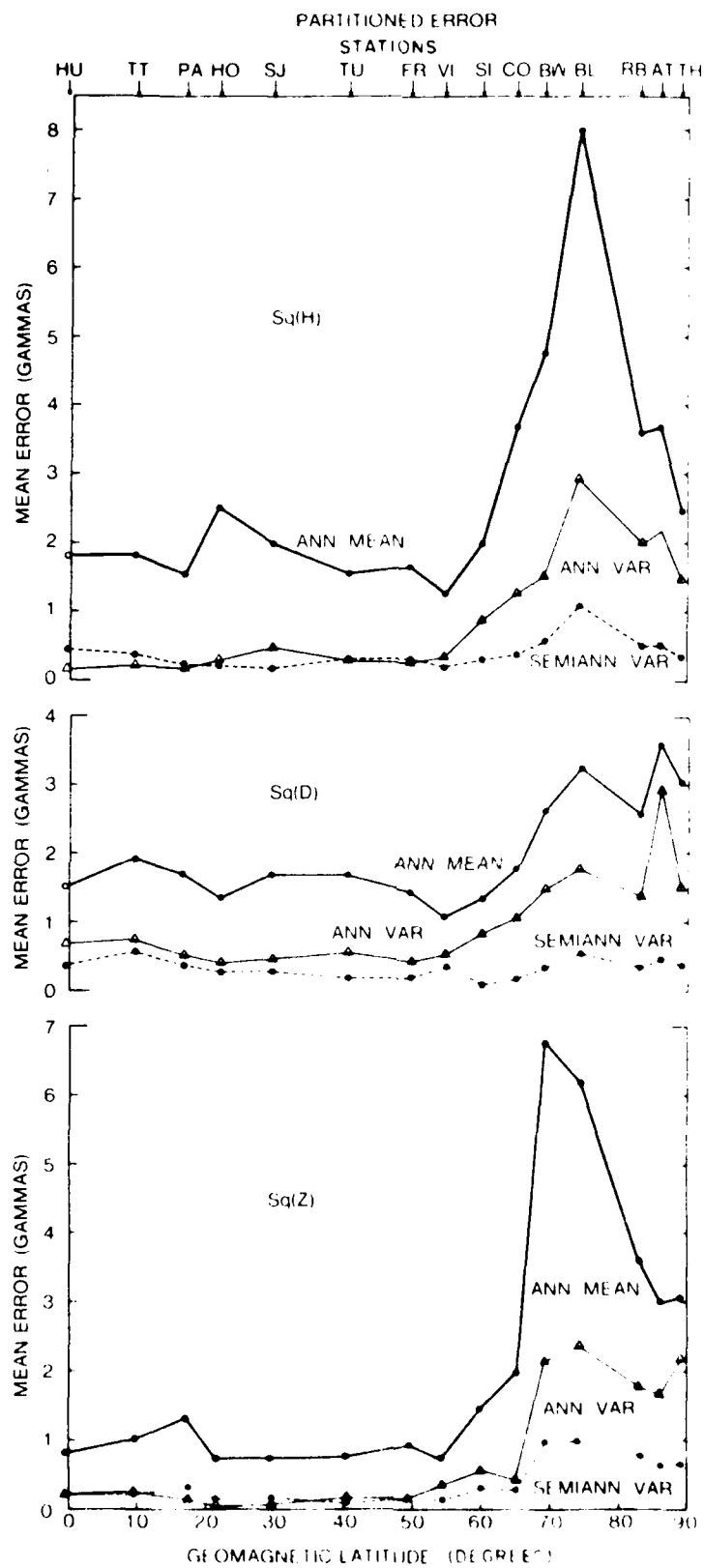


Figure 21

DAT
ILM